

## Research paper

## A Bertalanffy–Richards growth model perturbed by a time-dependent pattern, statistical analysis and applications<sup>☆</sup>

Antonio Di Crescenzo<sup>a</sup>, Paola Paraggio<sup>a,\*</sup>, Francisco Torres-Ruiz<sup>b,c</sup><sup>a</sup> Dipartimento di Matematica, Università di Salerno, 84084 Fisciano (SA), Italy<sup>b</sup> Departamento de Estadística e I.O., Facultad de Ciencias, Universidad de Granada, 18071 Granada, Spain<sup>c</sup> Instituto de Matemáticas de la Universidad de Granada (IMAG), Calle Ventanilla, 11, 18001 Granada, Spain

## ARTICLE INFO

## MSC:

60J70

62M05

60J80

## Keywords:

Richards growth model

Non-homogeneous birth–death process

Lognormal diffusion process

First-passage time

Maximum likelihood estimation

## ABSTRACT

We analyze a modification of the Richards growth model by introducing a time-dependent perturbation in the growth rate. This modification becomes effective at a special switching time, which represents the first-crossing-time of the Richards growth curve through a given constant boundary. The relevant features of the modified growth model are studied and compared with those of the original one. A sensitivity analysis on the switching time is also performed. Then, we define two different stochastic processes, i.e. a non-homogeneous linear birth–death process and a lognormal diffusion process, such that their means identify to the growth curve under investigation. For the diffusion process, we address the problem of parameters estimation through the maximum likelihood method. The estimates are obtained via meta-heuristic algorithms (namely, Simulated Annealing and Ant Lion Optimizer). A simulation study to validate the estimation procedure is also presented, together with a real application to oil production in France. Special attention is devoted to the approximation of switching time density, viewed as the first-passage-time density for the lognormal process.

## 1. Introduction

The Richards growth model is a generalization of the well-known logistic model. The main difference between the two models lays in symmetry properties of the resulting curves. Indeed, the logistic function has a symmetrical pattern with respect to the inflection point, in the sense that the carrying capacity (which is the limit value of the growth function) is twice the value of the curve in the inflection point. This behavior may not be particularly appropriate to describe some real phenomena which show asymmetrical growth patterns. For this reason, Richards in 1959 introduced a new growth curve that was called Richards growth curve (cf. Richards (1959) [1]). Some authors refer to it as Bertalanffy–Richards growth curve, since Richards extended previous works of Bertalanffy regarding plants growth. The flexibility of the afore-mentioned curve is another great advantage of the model. Indeed, for some particular choices of the involved parameters the most known growth functions (such as the Malthusian, the logistic and the Gompertz) can be obtained from the Richards curve. Nevertheless, if one refers to the classical representation of the curve, it is easy to note that the carrying capacity does not depend explicitly on the initial state. This feature may not be so realistic, since it is intuitive to believe that the maximum achievable value of a population size is influenced by the initial size. For this reason, a reformulation of the model that includes the initial size in the expression of the carrying capacity is useful.

<sup>☆</sup> This paper is dedicated to the cherished memory of our dear colleague and friend Patricia Román-Román.

\* Corresponding author.

E-mail addresses: [adicrescenzo@unisa.it](mailto:adicrescenzo@unisa.it) (A. Di Crescenzo), [pparaggio@unisa.it](mailto:pparaggio@unisa.it) (P. Paraggio), [fdeasis@ugr.es](mailto:fdeasis@ugr.es) (F. Torres-Ruiz).

The flexibility of the Richards deterministic model is also demonstrated by several applications in different fields which range from agricultural studies (such as in Hiroshima (2007) [2] and in Gerhard and Moltchanova (2022) [3]), to zoological studies (see for example Matis et al. (2011) [4], Nahashon (2006) [5], Köhn et al. (2007) [6], Lv et al. (2007) [7] and Russo et al. (2009) [8]) and to health sciences (cf. Macêdo et al. (2021) [9], Smirnova et al. (2022) [10] and Wang et al. (2012) [11]).

In order to include the randomness (which is typical in the phenomenological reality) in the description of the model, it is useful to introduce a stochastic counterpart of the considered growth curve. Typically, researchers define two classes of stochastic processes related to growth curves, that are the birth–death processes (e.g. Asadi et al. (2020) [12]) whose state-space is given by a discrete set and the diffusion processes (e.g. Román-Román et al. (2018) [13]) whose state-space is an interval of the real line. Both processes are usually constructed in such a way that the mean identifies with the corresponding deterministic curve. One of the main features of these “dynamic” models lays in their more accurate predictive capability with respect to the “static” deterministic models. Clearly, to perform real applications of these models, a good estimation of the involved parameters is required (see Dey et al. (2019) [14] where the problem of estimation of the Bertalanffy growth model is addressed). When the likelihood function is available in closed form, one can obtain the maximum likelihood estimates directly. However, this reasoning may lead to complex systems of non-linear equations which cannot be solved analytically. For this reason, as done elsewhere (see for example Di Crescenzo et al. (2022) [15], Hole et al. (2017) [16], Román-Román et al. (2015) [17] and Vera et al. (2008) [18]) we can adopt meta-heuristic optimization methods. In particular, the Simulated Annealing algorithm allows to obtain satisfactory estimates. In general, it is convenient making use of gradient free algorithms, especially when the expression of the derivative of the likelihood is intricate. In any case, since the parametric space  $\theta$  (which is the set containing all the possible values of the parameters) is in principle unbounded and continuous, it is better to provide a restriction of  $\theta$  based on the knowledge of the curve. In this way, we avoid unnecessary calculations and a long running time of execution of the algorithms.

The Richards growth model, as other competing models in this area, does not take into account external factors which may modify the growth rate at a certain time instant. For example, we may think about the oil production of a country. When the amount of produced oil decreases and crosses a fixed critical threshold, the government may decide to support new explorations in order to increase the quantity of extracted resources. As a further real example, we can refer to the evolution of some diseases in patients. In this case, when the monitoring parameters reach critical values, the medical team may consider to introduce a new therapy, whose effects is the stabilization of critical parameters and the reduction of the evolution of the disease. Inspired by these motivations, we would like to investigate the possible modifications of the classical Richards growth model in order to take into account the perturbations of the growth rate due to external factors that are effective from a certain moment on. Such modifications may lead to multi-sigmoidal growths, namely growths with multiple inflections. On the same line, a multi-sigmoidal version of the logistic model has been introduced in Di Crescenzo et al. (2022) [15] by increasing the number of the involved parameters. Instead, in the present work, the proposed modified curve and the classical one possess the same number of parameters. Indeed, the modification affects the time-dependence of one parameter. A similar study has been conducted recently to estimate the effect of a therapy on tumor dynamics described by Gompertz diffusion processes by Albano et al. (2015) [19]. The resulting modified model will be analyzed both from a deterministic and stochastic point of view. The problem of parameters estimation will be also addressed. A strategy to obtain the maximum likelihood estimates of the parameters involved in the definition of the corresponding diffusion process will be proposed.

The study introduces a time-dependent perturbation into the Richards growth model, offering an approach to take into account external factors affecting growth rates, which is effectively demonstrated through both theoretical analysis and practical applications, in particular the oil production in France. One of the strengths of this research lies in its comprehensive statistical analysis, employing meta-heuristic algorithms like Simulated Annealing and Ant Lion Optimizer for parameters estimation, thus ensuring robust results validated by simulation studies. The structure of the paper is organized as follows. In Section 2, the classical deterministic Richards growth model is introduced. Several features of the model are analyzed, such as the limit behavior with respect to the parameters, the inflection point, the approximation of the curve with a straight line near the inflection point and the first-crossing-time problem. In Section 3, we consider a modification of the classical Richards growth model, by adding a time dependent function to one of the relevant parameters. Such modification, whose consequences are visible after a certain time, called critical or switching time, affects the growth rate which becomes, under suitable conditions, greater than the previous one. The resulting deterministic curve is then studied and a sensitivity analysis on the switching time is also considered. In Sections 4 and 5, the stochastic counterparts of the proposed models are introduced. In detail, we first consider two different special time-inhomogeneous birth–death processes following the line of Majee et al. (2022) [20]. Sufficient and necessary conditions are provided in order to have a mean of the birth–death processes of modified Richards type. Moreover, in order to have a more manageable stochastic counterpart, we define two lognormal diffusion processes whose means are of Richards and modified Richards type, respectively. Some comparisons between the two diffusion processes are also provided. In particular, one of them turns out to be very useful for the estimation of the modified model. The problem of parameters estimation is addressed in Section 6. A procedure to estimate the modified process is described. The relevant parameters are estimated by means of maximum likelihood method since an explicit expression of the log-likelihood function is available. This function is maximized via meta-heuristic algorithms, in particular Simulated Annealing and Ant Lion Optimizer are used in Section 7. A simulation study to validate the described procedures ends the estimation study in Section 8. Finally, an application to real data regarding oil production in France is studied in Section 9.

## 2. The Richards growth curve

The Bertalanffy–Richards growth curve  $x_\theta(t)$ ,  $t \geq t_0$ , is given by (cf. Román-Román et al. (2015) [17])

$$x_\theta(t) = x_0 \left( \frac{\eta + k^{t_0}}{\eta + k^t} \right)^q, \quad t \geq t_0, \tag{1}$$

where  $\theta := (q, k, \eta)^T$  is the vector of the parameters with  $q > 0$ ,  $0 < k < 1$  and  $\eta > 0$ . The function (1) is a generalization of the logistic growth curve which can be obtained for  $q = 1$ . The main difference between Eq. (1) and the logistic model lays in the behavior of the curve at the inflection point. Indeed, the value at inflection point of the logistic model equals a half of the carrying capacity (namely the asymptotic value of a growth curve) whereas the one of Bertalanffy–Richards is equal to a (possibly) different fraction of the carrying capacity. In particular, the carrying capacity of (1) depends explicitly on the initial value  $x_0$ . Indeed, it is given by

$$\mathcal{K}_\theta := \lim_{t \rightarrow +\infty} x_\theta(t) = x_0 \left( 1 + \frac{k^{t_0}}{\eta} \right)^q. \tag{2}$$

The function (1), is the solution of a particular inhomogeneous Malthusian equation having a time-dependent growth rate  $h_\theta(t)$ , i.e.

$$\frac{d}{dt} x_\theta(t) = h_\theta(t) x_\theta(t), \quad t \geq t_0, \quad x_\theta(t_0) = x_0, \tag{3}$$

where

$$h_\theta(t) := q \frac{k^t |\log k|}{\eta + k^t}. \tag{4}$$

It is not hard to see that the growth rate  $h_\theta(t)$  is a positive and decreasing function for  $t \geq t_0$ . The function  $x_\theta(t)$  is also the solution of a particular differential equation in which the time dependence of the right-hand-side is expressed only through  $x_\theta(t)$ , i.e.

$$\frac{d}{dt} x_\theta(t) = q |\log k| x_\theta(t) \left[ 1 - \frac{\eta}{\eta + k^{t_0}} \left( \frac{x_\theta(t)}{x_0} \right)^{1/q} \right], \quad t \geq t_0. \tag{5}$$

Note that when  $\eta \rightarrow +\infty$ ,  $q \rightarrow +\infty$  and  $\left( \frac{\eta}{\eta + k^{t_0}} \right)^q \rightarrow \frac{x_0}{\mathcal{K}_\theta}$ , Eq. (5) becomes

$$\frac{d}{dt} x_\theta(t) = |\log k| x_\theta(t) \log \frac{\mathcal{K}_\theta}{x_\theta(t)}, \quad t \geq t_0,$$

which is a particular Gompertz equation having a carrying capacity given by  $\mathcal{K}_\theta$ .

**Remark 2.1.** Without loss of generality, it is possible to take  $t_0 = 0$ . Indeed, by setting  $t' := t - t_0$ , we get a model of the same type of (1). Precisely,

$$x_\theta(t) = x_0 \left( \frac{\eta + k^{t_0}}{\eta + k^t} \right)^q = x_0 \left( \frac{\hat{\eta} + 1}{\hat{\eta} + k^{t'}} \right)^q =: y_\theta(t'), \quad t' \geq 0,$$

where  $\hat{\eta} := \eta/k^{t_0}$ . We point out that the parameter  $k$  is the same for both the models.

In Table 1, we provide some limit behaviors of the proposed growth model (in agreement with the results given by Albano et al. (2022) [21]). Note that for  $\eta \rightarrow 0^+$ , the Richards curve  $x(t)$  converges to a Malthusian growth curve.

### 2.1. Inflection point and related quantities

The inflection point  $t_I$  of the Bertalanffy–Richards curve (1) has an explicit expression given by

$$t_I = \frac{\log(\eta/q)}{\log k}, \quad x_\theta(t_I) = \mathcal{K}_\theta \left( \frac{q}{1+q} \right)^q. \tag{6}$$

See Fig. 1 for some plots of the Bertalanffy–Richards growth curve.

From Eq. (6), we note that the ratio between  $x_\theta(t_I)$  and the carrying capacity (2) depends only on  $q$ , and it is given by  $\left( \frac{q}{1+q} \right)^q$ . In the logistic case (obtained for  $q = 1$ ), this fraction is equal to  $1/2$ . Moreover, one has  $t_I > t_0$  if and only if  $\eta < qk^{t_0}$ . Now, we can provide an interpretation of the relevant parameters of the model, i.e.  $\theta = (q, k, \eta)^T$ . It turns out that

- The parameter  $q$  affects the ratio between the carrying capacity  $\mathcal{K}_\theta$  of the model and the inflection point  $x_\theta(t_I)$ . Indeed, the ratio  $\mathcal{K}_\theta/x_\theta(t_I) = (1 + 1/q)^q$  is increasing in  $q > 0$ .
- The parameter  $\eta$  represents a measure of the distance between  $x_\theta(t)$  and the exponential function  $x_0 k^{-qt}$ . Indeed, the bigger  $\eta$  is, the further the function  $x_\theta(t)$  is from being the exponential function  $x_0 k^{-qt}$  (see also Fig. 2). In particular, as shown in Table 2, for  $\eta \rightarrow 0^+$  the function  $x_\theta(t)$  converges to  $x_0 k^{-qt}$ .
- The parameter  $k$  affects the value of the inflection point  $t_I$ . Indeed, for  $\eta < qk^{t_0}$  the value of  $t_I$  increases for increasing  $k$ .

**Table 1**  
The growth equation, the growth function and the carrying capacity of the model (3) under the specified limit conditions, where  $x'_\theta(t) = \frac{d}{dt}x_\theta(t)$ .

Case no.	Limit conditions	Growth equation
1	$k \rightarrow 0^+$	$x'_\theta(t) = 0$
2	$k \rightarrow 1^-$	$x'_\theta(t) = 0$
3	$\eta \rightarrow 0^+$	$x'_\theta(t) = q  \log k  x_\theta(t)$
4	$q \rightarrow 0^+$	$x'_\theta(t) = 0$
5	$q \rightarrow 1$	$x'_\theta(t) = \frac{k'  \log k }{\eta + k'} x_\theta(t)$
6	$\eta, q \rightarrow +\infty, \left(\frac{\eta}{\eta + k^t}\right)^q \rightarrow \frac{x_0}{\mathcal{K}_\theta}$	$x'_\theta(t) =  \log k  x_\theta(t) \log \frac{\mathcal{K}_\theta}{x_\theta(t)}$
Case no.	Growth function	Carrying capacity
1	$x_\theta(t) = x_0$	$x_0$
2	$x_\theta(t) = x_0$	$x_0$
3	$x_\theta(t) = x_0 k^{-qt}$	$+\infty$
4	$x_\theta(t) = x_0$	$x_0$
5	$x_\theta(t) = x_0 \left(\frac{\eta + k^{t_0}}{\eta + k^t}\right)$	$x_0 \left(\frac{\eta + k^{t_0}}{\eta}\right)$
6	$x_\theta(t) = \mathcal{K}_\theta \exp[-\log(\mathcal{K}_\theta/x_0)e^{\log k(t-t_0)}]$	$\mathcal{K}_\theta$

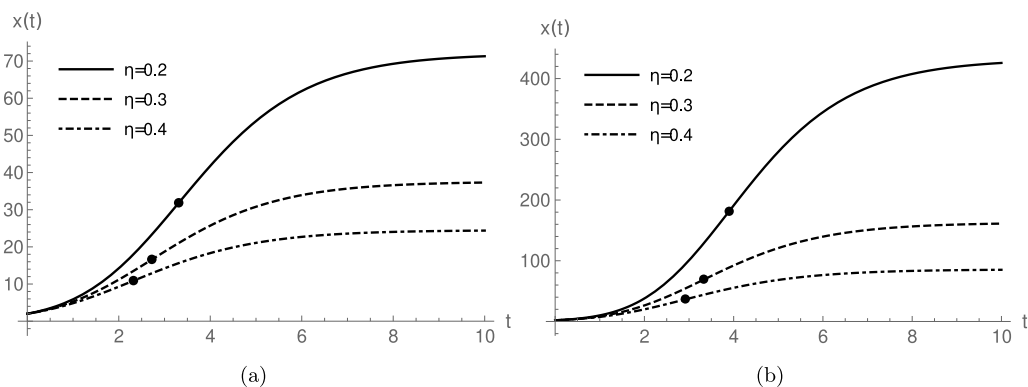


Fig. 1. The function  $x_\theta(t)$  and the inflection point  $t_I$  (dot) given in Eq. (6) with  $t_0 = 0, x_0 = 2, k = 0.5, \eta = 0.2, 0.3, 0.4$  and (a)  $q = 2$  and (b)  $q = 3$ .

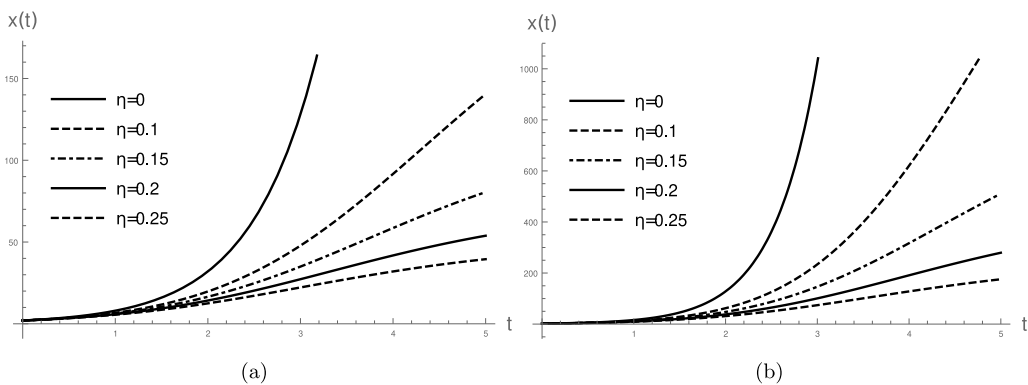


Fig. 2. The function  $x_\theta(t)$  with  $t_0 = 0, x_0 = 2, k = 0.5$ , (a)  $q = 2$  and (b)  $q = 3$  for  $\eta = 0, 0.1, 0.15, 0.2, 0.25$ .

As already done in other similar researches (see, for example, Asadi et al. (2020) [12] and Di Crescenzo et al. (2022) [15]), we can analyze the behavior of the growth curve  $x_\theta(t)$  around the inflection point  $t_I$  by using a linear approximation. With this aim, we consider the maximum specific growth rate, denoted by  $\mu$ , which is the slope of the line tangent to  $x_\theta(t)$  in  $t_I$  and the lag time  $\lambda$  which is the intersection between the  $x$ -axis and the tangent. For the Bertalanffy–Richards curve, these quantities are given by

$$\mu = (\eta + k^{t_0})^q \frac{x_0 |\log k|}{\eta^q} \left(\frac{q}{q+1}\right)^{q+1} > 0, \quad \lambda = t_I - \frac{1 + 1/q}{|\log k|} < t_I.$$

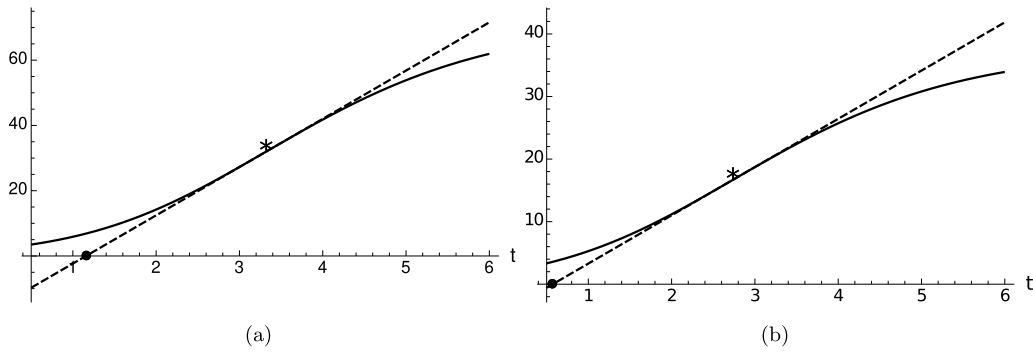


Fig. 3. The function  $x_\theta(t)$  (solid line), the line tangent to the curve (dashed line), the inflection point (star point) and the lag time (dot point) in  $t_I$  (dot) with  $t_0 = 0$ ,  $x_0 = 2$ ,  $k = 0.5$ ,  $q = 2$  and (a)  $\eta = 0.2$  and (b)  $\eta = 0.3$ . In (a)  $\mu \simeq 14.79$  and  $\lambda \simeq 1.16$ . In (b)  $\mu \simeq 7.71$  and  $\lambda \simeq 0.57$ .

Note that if  $k \rightarrow 1$  or  $q \rightarrow 0$ , then  $\mu$  tends to 0 and thus the tangent line tends to be parallel to the  $x$ -axis. Indeed, in these limit cases the curve  $x_\theta(t)$  degenerates into a horizontal line. In Fig. 3, we provide the plot of the line tangent to the Bertalanffy–Richards curve at the inflection time instant  $t_I$ .

### 2.2. Threshold crossing problem

In this section, we consider the problem of first crossing time. Let  $B(t)$  be a time-dependent boundary given by

$$B(t) := (1 + p)x_\theta(t), \quad t \geq t_0, \quad p > 0.$$

The corresponding first crossing time  $\theta_t$  for a fixed time instant  $t$  is then defined as follows

$$\theta_t := \min\{s \geq t_0 : x_\theta(s) = B(t)\},$$

and it represents the first instant in which the growth curve  $x_\theta(t)$  crosses the threshold  $B(t)$ . Clearly, if  $B(t)$  is greater than the carrying capacity, the set  $\{s \geq t_0 : x_\theta(s) = B(t)\}$  is empty and then  $\theta_t := +\infty$ . Otherwise,  $\theta_t$  is finite and it can be explicitly determined. The expression one gets is the following

$$\theta_t = \frac{1}{\log k} \log \left( \frac{\eta + k^t}{(1 + p)^{1/q}} - \eta \right) = t_I + \frac{\log \left( \frac{q(\eta + k^t)}{\eta(1 + p)^{1/q}} - q \right)}{\log k}.$$

Note that when  $t = t_0$ , then  $B(t_0) = (1 + p)x_0 > x_0$  and

$$\theta_{t_0} = \frac{\log \left( \frac{\eta + k^{t_0}}{(1 + p)^{1/q}} - \eta \right)}{\log k}.$$

Moreover, when  $t = t_I$ , then the boundary is

$$S := B(t_I) = (1 + p)x_\theta(t_I) \tag{7}$$

and the corresponding first crossing time is given by

$$t^* := \theta_{t_I} = t_I + \frac{\log \left( \frac{1 + q}{(1 + p)^{1/q}} - q \right)}{\log k} > t_I. \tag{8}$$

### 3. A modified model

Once the parameters of the model are set, the evolution of the growth curve follows the resulting pattern and no further modifications are considered. On the other hand, there are several real situations in which the growth rate may be modified due to the presence of external factors. Usually, the effects produced by external modifications become significant starting from a critical time. As an example, think about the case of oil production of a country: when the quantity of produced oil is lower than a fixed threshold, the government may decide to support new explorations aiming to increase the amount of production.

For this reason we consider a modified version of the classical Bertalanffy–Richards growth curve by introducing a time-varying term into the growth rate  $h_\theta(t)$  of the Malthusian Eq. (3). Specifically, in Eq. (1) we substitute the parameter  $q$  with a time-dependent one defined as

$$\tilde{q}(t) := \begin{cases} q, & t_0 \leq t \leq t^* \\ q + C(t), & t > t^*, \end{cases} \tag{9}$$

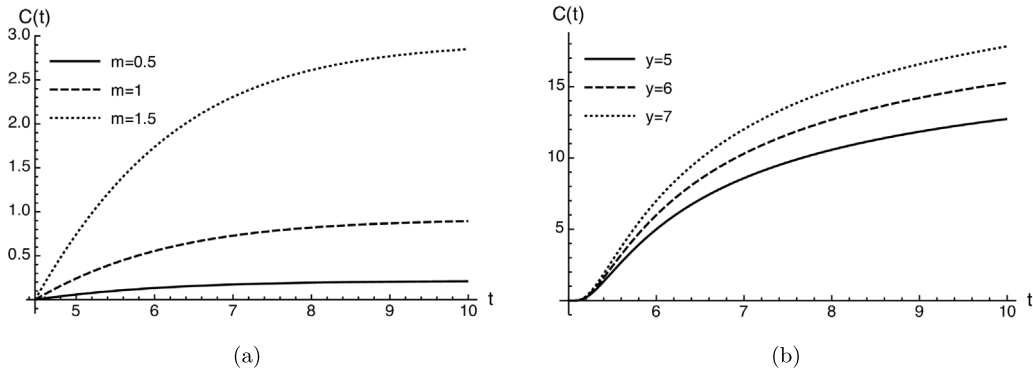


Fig. 4. (a) The function  $C(t)$  given in Eq. (12) with  $m = 0.5, 1, 1.5$ ,  $p = 0.3$ ,  $t_0 = 0$ ,  $x_0 = 2$ . (b) The function  $C(t)$  given in Eq. (13) with  $y = 5, 6, 7$ ,  $\alpha = 1$ ,  $\beta = 0.75$ ,  $p = 0.8$ . In both cases, we have  $k = 0.5$ ,  $\eta = 0.2$ ,  $q = 2$ .

where  $t^* \geq t_0$  and  $C(t)$  is a continuous, bounded and positive function with  $\lim_{t \rightarrow t^*} C(t) = 0$ .

Hence, the growth rate  $\tilde{h}_\theta(t)$  of the new model is given by

$$\tilde{h}_\theta(t) = \frac{\tilde{q}(t)}{q} h_\theta(t) = \tilde{q}(t) \frac{k^t |\log k|}{\eta + k^t}, \quad t \geq t_0. \tag{10}$$

From now on, we consider  $t^* > t_I$  as the time instant defined in Eq. (8). Note that the conditions verified by the function  $C(t)$  ensure the continuity of the function  $\tilde{q}(t)$  and consequently of the function  $\tilde{h}_\theta(t)$ . It can be also noticed that the adoption of the new term given in (9) increases the growth rate, indeed

$$\tilde{h}_\theta(t) - h_\theta(t) = C(t) \frac{k^t |\log k|}{\eta + k^t} > 0, \quad t \geq t^*.$$

Let us denote by  $\tilde{x}_\theta(t)$  the corresponding growth curve, which is the solution of Eq. (3) where the function  $h_\theta(t)$  is replaced by  $\tilde{h}_\theta(t)$ . In particular, we have that for any  $t \geq t_0$

$$\begin{aligned} \tilde{x}_\theta(t) &= x_\theta(t) \exp\left(\int_{t^*}^{\max\{t, t^*\}} C(s) \frac{k^s |\log k|}{\eta + k^s} ds\right) \\ &= \begin{cases} x_\theta(t), & t_0 \leq t < t^* \\ x_\theta(t) \exp\left(\int_{t^*}^t C(s) \frac{k^s |\log k|}{\eta + k^s} ds\right), & t \geq t^*. \end{cases} \end{aligned} \tag{11}$$

We remark that  $\tilde{x}_\theta(t) \geq x_\theta(t)$  for any  $t \geq t_0$ . The carrying capacity of the new growth curve (11) is given by

$$\tilde{\mathcal{K}}_\theta = \mathcal{K}_\theta \exp\left(\int_{t^*}^{+\infty} C(s) \frac{k^s |\log k|}{\eta + k^s} ds\right) > \mathcal{K}_\theta,$$

where  $\mathcal{K}_\theta$  is given in Eq. (2).

**Example 3.1.** Fig. 4(a) provides some plots of  $C(t)$ , where

$$C(t) = \left(\frac{1}{\eta + k^t}\right)^m - \left(\frac{1}{\eta + k^{t^*}}\right)^m, \quad t \geq t^*, \tag{12}$$

with  $m > 0$ . In this case the function  $C(t)$  has a downward concavity, for any  $t \geq t^*$ . In Fig. 5(a) the behavior of the corresponding modified model  $\tilde{x}_\theta(t)$  is shown.

A different case is shown in Fig. 4(b) where

$$C(t) = y \exp\left(\frac{\alpha}{\beta} [1 - (t - t^*)^{-\beta}]\right), \quad t > t^*, \tag{13}$$

with  $y, \alpha, \beta > 0$ . In this case, the function  $C(t)$  has a sigmoidal behavior. Fig. 5(b) illustrates the behavior of the corresponding modified model  $\tilde{x}_\theta(t)$ , which is multi-sigmoidal with multiple inflections.

In general, since  $C(t)$  is a bounded function, one has  $\tilde{\mathcal{K}}_\theta < +\infty$ . The difference between the original curve  $x_\theta(t)$  and the modified one  $\tilde{x}_\theta(t)$  becomes more and more relevant after the time instant  $t^*$ . Indeed, for  $t_0 < t \leq t^*$  it results  $\tilde{x}_\theta(t) = x_\theta(t)$ , whereas for  $t > t^*$

$$\frac{d}{dt} [\tilde{x}_\theta(t) - x_\theta(t)] = x_\theta(t) \left[ \tilde{h}_\theta(t) \exp\left(\int_{t^*}^t C(s) \frac{k^s |\log k|}{\eta + k^s} ds\right) - h_\theta(t) \right] > 0.$$

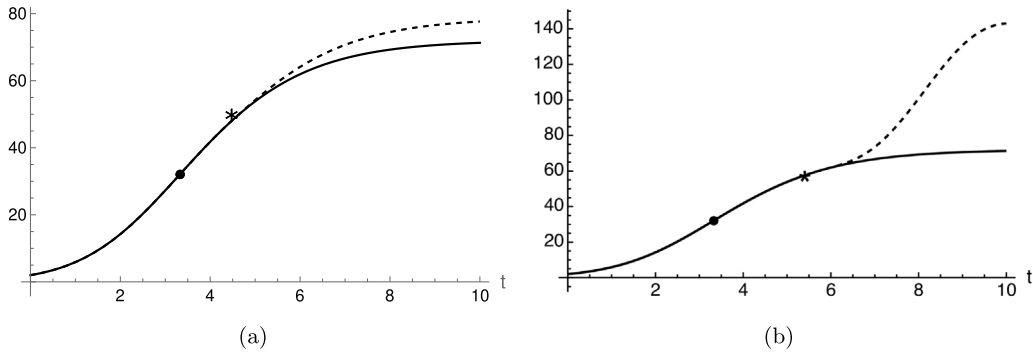


Fig. 5. The Bertalanffy–Richards curve (solid line) and the modified curve (dashed line) (a) for  $C(t)$  given in Eq. (12) with  $p = 0.3, m = 1$  and (b) for  $C(t)$  given in Eq. (13) with  $p = 0.8, y = 2, \alpha = 4, \beta = 0.5$ . In both cases  $\eta = 0.2, t_0 = 0, x_0 = 2, k = 0.5, q = 2$ . The dots and the star points represent the inflection point at  $t_i$  and the point at  $t^*$ , respectively.

**Remark 3.1.** Similarly as Remark 2.1, also for the modified model (11) one can take  $t_0 = 0$  without loss of generality. Indeed, by setting  $\hat{C}(t') := C(t)$  with  $t' := t - t_0, \hat{t}^* := t^* - t_0$  and  $\hat{\eta} := \eta/k^{t_0}$  we have

$$\begin{aligned} \tilde{x}_\theta(t) &= x_0 \left( \frac{\eta + k^{t_0}}{\eta + k^t} \right)^q \exp \left( \int_{t^*}^t C(s) \frac{k^s |\log k|}{\eta + k^s} ds \right) \\ &= x_0 \left( \frac{\hat{\eta} + 1}{\hat{\eta} + k^{t'}} \right)^q \exp \left( \int_{\hat{t}^*}^{t'} \hat{C}(s') \frac{k^{s'} |\log k|}{\hat{\eta} + k^{s'}} ds' \right) =: \hat{y}_\theta(t'), \quad t' \geq 0. \end{aligned}$$

It is easy to note that the curve  $\hat{y}_\theta(t')$  is of the same type of (11).

### 3.1. Sensitivity analysis

In this section we analyze the consequences of a perturbation on the time instant  $t^*$  involved in the definition of the modified growth curve  $\tilde{x}_\theta(t)$ . Hereafter, we will denote the modified curve by  $\tilde{x}_\theta^{t^*}$  and the modified function  $C_{t^*}(t)$  to point out their dependence on the time instant  $t^*$ . To perform the sensitivity analysis, we expand  $\tilde{x}_\theta^{t^*+\epsilon}$  in a Taylor series centered in  $t^*$  with  $\epsilon > 0$ . Therefore, one has

$$\tilde{x}_\theta^{t^*+\epsilon} - \tilde{x}_\theta^{t^*} = \epsilon \cdot \frac{\partial}{\partial t^*} \tilde{x}_\theta^{t^*} + o(\epsilon)$$

with  $\lim_{\epsilon \rightarrow 0^+} \frac{o(\epsilon)}{\epsilon} = 0$ . Since

$$\frac{\partial}{\partial t^*} \tilde{x}_\theta^{t^*}(t) = \tilde{x}_\theta^{t^*}(t) \cdot \int_{t^*}^t \left( \frac{\partial}{\partial t^*} C_{t^*}(s) \right) \frac{k^s |\log k|}{\eta + k^s} ds, \quad t > t^*,$$

we have that

$$\text{sgn} \left( \tilde{x}_\theta^{t^*+\epsilon} - \tilde{x}_\theta^{t^*} \right) = \text{sgn} \left( \int_{t^*}^t \left( \frac{\partial}{\partial t^*} C_{t^*}(s) \right) \frac{k^s |\log k|}{\eta + k^s} ds \right), \quad t > t^*.$$

Whereas,  $\tilde{x}_\theta^{t^*+\epsilon} - \tilde{x}_\theta^{t^*} = 0$  for  $t \leq t^*$ . As an example, in Fig. 6 we plot the modified curve  $\tilde{x}_\theta(t)$  and the effect of the perturbation for  $\epsilon = 0.5$  and for the function  $C(t)$  given in Eq. (12). The curve  $\tilde{x}_\theta^{t^*+\epsilon}$  goes down as the parameter  $\epsilon$  increases since the derivative of  $C(t)$  with respect to  $t^*$  is negative.

## 4. A special linear birth–death process

In this section, we introduce an evolutionary model based on the birth–death process introduced in Majee et al. (2022) [20]. In more detail, we suppose that the population size can be described by an inhomogeneous linear birth–death process  $\{X(t); t \geq 0\}$  with state-space  $\mathbb{N}_0 = \{0, 1, 2, \dots\}$  where the state 0 is an absorbing endpoint. The existence of an absorbing endpoint reflects the situations in which the extinction of the population may occur. Moreover, we consider a positive and integrable function on  $(0, t)$  for any  $t > 0$ , denoted by  $\lambda(t)$  ( $\mu(t)$ ), which represents the individual birth (death) rate at time  $t$ . Since in real populations there are some individuals who have no reproduction power, we denote by  $\rho(t) \in [0, 1]$  this portion evaluated at time  $t$ . We assume that  $\rho(t)$  is time-varying, since the reproduction power of individuals may change over time, due to diseases or other natural reasons. Therefore, the individual transition rates of this special birth–death process are given by

$$\lambda(t) := (1 - \rho(t))\lambda, \quad \mu(t) := \mu,$$

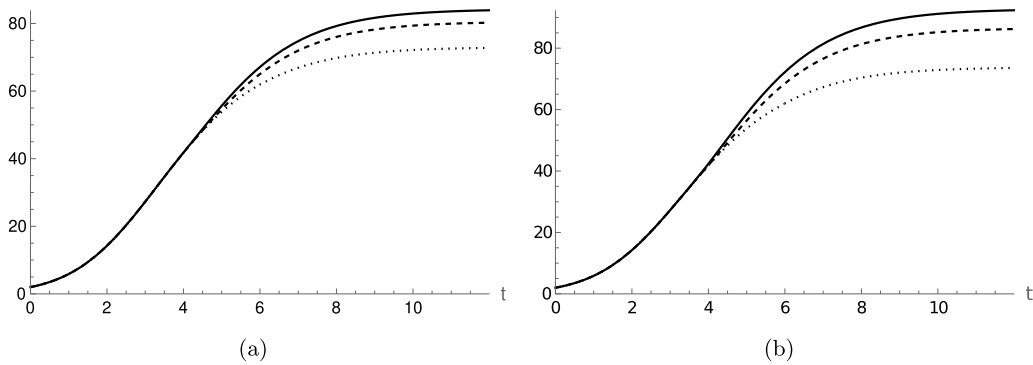


Fig. 6. The modified Bertalanffy–Richards curve  $\tilde{x}_\theta^+$  (solid line) and the perturbed ones  $\tilde{x}_\theta^{+\varepsilon}$  (dashed and dotted lines) for  $x_0 = 2$ ,  $\eta = 0.2$ ,  $k = 0.5$ ,  $t_0 = 0$ ,  $q = 2$ ,  $m = 1$ , (a)  $p = 0.3$  and (b)  $p = 0.1$  with  $\varepsilon = 0.3$  (dashed) and  $\varepsilon = 2$  (dotted).

where  $\lambda, \mu > 0$  and  $\rho(t) \in [0, 1]$  is an integrable function over any interval  $(0, \bar{t})$  for  $\bar{t} > 0$ .

Hence, the transition rates are

$$\begin{aligned} \lambda_n(t) &:= \lim_{h \rightarrow 0^+} \frac{1}{h} \mathbb{P}[X(t+h) = n+1 \mid X(t) = n] = n\lambda(t) = n(1 - \rho(t))\lambda, & n \in \mathbb{N}_0, \\ \mu_n(t) &:= \lim_{h \rightarrow 0^+} \frac{1}{h} \mathbb{P}[X(t+h) = n-1 \mid X(t) = n] = n\mu(t) = n\mu, & n \in \mathbb{N}. \end{aligned} \tag{14}$$

We denote by

$$P_{yx}(t) = \mathbb{P}[X(t) = x \mid X(0) = y], \quad t \geq 0,$$

the probability that the birth–death process  $X(t)$  is in the state  $x$  at the time  $t$ , conditional on the initial state  $X(0) = y \in \mathbb{N}$ . As shown in Tan (1986) [22], the probability generating function of  $X(t)$  has the following expression

$$G(z, t) = \left\{ 1 - (z-1)[(z-1)\phi(t) - \psi(t)]^{-1} \right\}^y, \quad 0 < z < 1, t \geq 0,$$

where

$$\begin{aligned} \psi(t) &= \exp\left(t(\mu - \lambda) + \lambda \int_0^t \rho(\tau) d\tau\right), \\ \phi(t) &= \lambda \int_0^t (1 - \rho(\tau)) \exp\left(\tau(\mu - \lambda) + \lambda \int_0^\tau \rho(s) ds\right) d\tau, \quad t \geq 0. \end{aligned}$$

In the following proposition, we provide a sufficient and necessary condition so that the birth–death process  $X(t)$  has a modified Bertalanffy–Richards conditional mean.

**Proposition 4.1.** *The linear birth–death process with birth and death rates given by*

$$\lambda_n(t) = n\lambda(t), \quad \mu_n = n\mu(t), \quad t \geq 0,$$

with  $\lambda(t)$  and  $\mu(t)$  defined in Eqs. (14), has conditional mean

$$E_y(t) := \mathbb{E}[X(t) \mid X(0) = y] = y \left( \frac{\eta + 1}{\eta + k^t} \right)^q \exp\left( \int_{t^*}^{\max\{t, t^*\}} C(s) \frac{k^s |\log k|}{\eta + k^s} ds \right), \quad t \geq 0,$$

if, and only if,

$$1 - \rho(t) = \frac{\mu + \tilde{h}_\theta(t)}{\lambda}, \quad t \geq 0, \tag{15}$$

with  $\lambda - \mu = -q \log k > 0$  and  $\tilde{h}_\theta(t)$  given in Eq. (10).

**Proof.** The conditional mean  $E_y(t)$  satisfies the following differential equation

$$\frac{d}{dt} E_y(t) = (\lambda(t) - \mu(t)) E_y(t), \quad t \geq 0.$$

On the other hand, the modified Bertalanffy–Richards function  $\tilde{x}_\theta(t)$  verifies the differential Eq. (5) with time-dependent growth rate  $\tilde{h}_\theta(t)$ . So, the function  $\rho(t)$  must be chosen as in Eq. (15).  $\square$

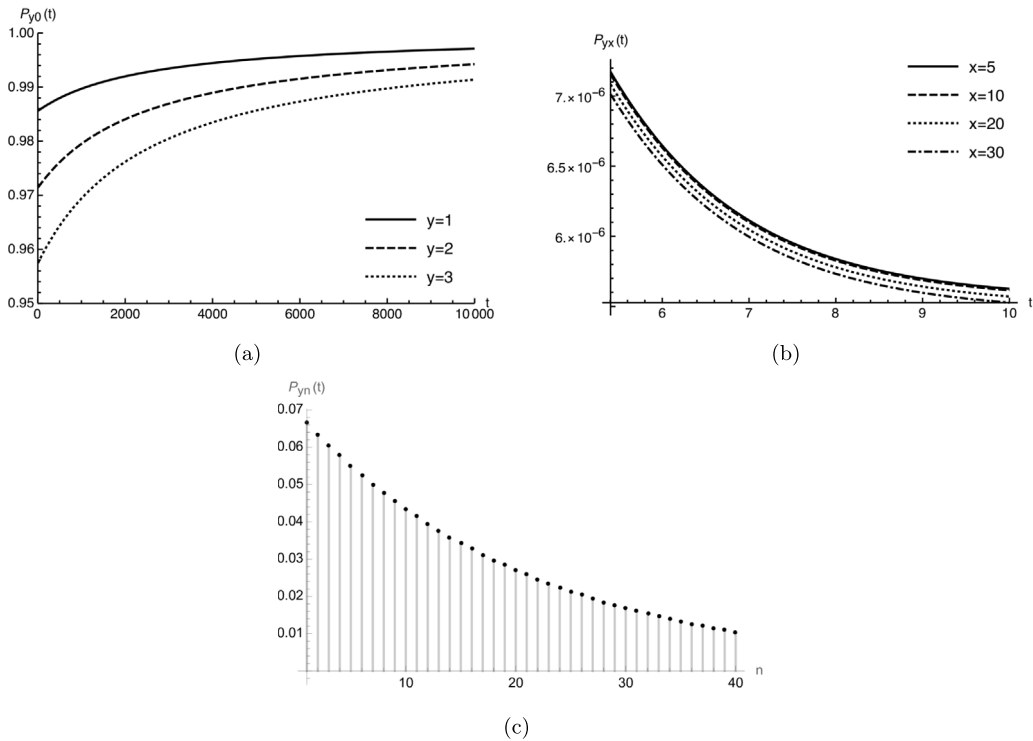


Fig. 7. The transition probabilities (a)  $P_{y0}(t)$ , (b)  $P_{yx}(t)$  as a function of  $t$  and (c)  $P_{yn}(t)$  as a function of  $n$  for  $C(t)$  defined in Eq. (12), with  $\eta = 0.2$ ,  $m = 1$ ,  $k = 0.5$ ,  $q = 2$ ,  $p = 0.8$ . In (a), one has  $\mu = 1$ ,  $y = 1, 2, 3$ . In (b), one has  $\mu = 1$ ,  $y = 1$  and  $x = 5, 10, 20, 30$ . In (c), one has  $\mu = 0.01$ ,  $t = 6$  and  $y = 1$ .

From now on, we will assume that the condition (15) holds. Consequently,

$$\begin{aligned} \psi(t) &= \left(\frac{\eta + k^t}{\eta + 1}\right)^q \exp\left(\int_{t^*}^{\max\{t, t^*\}} C(s) \frac{k^s \log k}{\eta + k^s} ds\right), \\ \phi(t) &= -\exp\left(-\int_0^t \tilde{h}_\theta(u) du\right) + \mu \int_0^t \exp\left(-\int_0^s \tilde{h}_\theta(u) du\right) ds, \quad t \geq 0. \end{aligned} \tag{16}$$

As shown in Tan (1986) [22], the transition probabilities and the conditional variance of the process can be expressed as follows, for any  $t \geq 0$ ,

$$\begin{aligned} P_{y0}(t) &= \left(1 - \frac{1}{\psi(t) + \phi(t)}\right)^y, \\ P_{yx}(t) &= \left(\frac{\phi(t)}{\psi(t) + \phi(t)}\right)^x \sum_{i=0}^{\min(x,y)} \binom{y}{i} \binom{y+x-i-1}{y-1} (\phi(t)^{-1} - 1)^i \left(1 - \frac{1}{\psi(t) + \phi(t)}\right)^{y-i} \end{aligned}$$

and

$$Var_{y,y}(t) := \text{Var}[X(t) | X(0) = y] = y \frac{\psi(t) + 2\phi(t) - 1}{\psi^2(t)}.$$

Some plots of the transition probabilities are provided in Fig. 7 for various choices of the parameters. In these cases, the probability  $P_{y0}(t)$  is increasing with respect to  $t$ , whereas the probability  $P_{yn}(t)$  is decreasing with respect both to  $t$  and  $n$ . It is worth to notice that, since  $\tilde{\psi} := \lim_{t \rightarrow +\infty} \psi(t) < +\infty$  and  $\tilde{\phi} := \lim_{t \rightarrow +\infty} \phi(t) = +\infty$ , the probability of an ultimate extinction is equal to 1, indeed

$$\pi_{y0} := \lim_{t \rightarrow +\infty} P_{y0}(t) = \left(1 - \frac{1}{\tilde{\psi} + \tilde{\phi}}\right)^y = 1.$$

See Fig. 8 for some plots of the conditional variance. Note that since the conditional variance is bounded, the conditional mean is a significant statistic for the process.

#### 4.1. A special time-inhomogeneous linear birth process

In Section 4 we considered a birth–death process with time-dependent transition rates and we investigated the conditions under which its mean is of modified Bertalanffy–Richards type. Since the growth curve  $\tilde{x}_\theta(t)$  may be significantly different from the sample

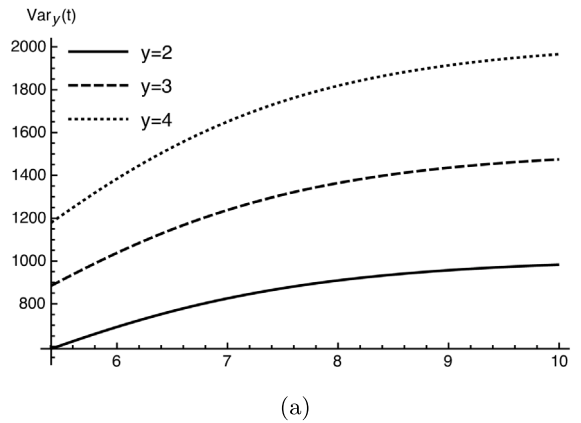


Fig. 8. The conditional variance  $Var_y(t)$  as a function of  $t$  with  $\eta = 0.2$ ,  $m = 1$ ,  $k = 0.5$ ,  $q = 2$ ,  $\mu = 0.01$ ,  $p = 0.8$  and  $y = 2, 3, 4$ .

paths of the birth–death process (because of the presence of an absorbing endpoint), we now propose a stochastic process  $X(t)$  more suitable to describe a growth phenomenon by removing the possibility of having downward jumps (deaths). Under this assumption, the individual transition rates of  $X(t)$  are given by

$$\lambda(t) := (1 - \rho(t))\lambda, \quad \mu(t) := 0, \tag{17}$$

where  $\lambda > 0$  and  $0 \leq \rho(t) \leq 1$  is an integrable function over the interval  $(0, t)$ . Hence, the state-space of the process is given by  $S := \{y, y + 1, \dots\}$  being  $P[X(0) = y] = 1$ . The result of Proposition 4.1 can be updated to this special case as shown in the following

**Proposition 4.2.** *The linear birth process with birth rate*

$$\lambda_n = n\lambda(t), \quad t \geq 0 \tag{18}$$

with  $\lambda(t)$  given in Eq. (17), has conditional mean

$$E_y(t) = E[X(t) | X(0) = y] = y \left( \frac{\eta + 1}{\eta + k^t} \right)^q \exp \left( \int_{t^*}^{\max\{t, t^*\}} C(s) \frac{k^s |\log k|}{\eta + k^s} ds \right), \quad t \geq 0, \tag{19}$$

if, and only if,

$$1 - \rho(t) = \frac{\tilde{h}_\theta(t)}{\lambda}, \quad t \geq 0,$$

with  $\lambda = -q \log k > 0$  and  $\tilde{h}_\theta(t)$  given in Eq. (10).

In this case, considering the birth rate given in Eq. (18), the transition probabilities can be expressed as

$$P_{yx}(t) = P[X(t) = x | X(0) = y] = \binom{x-1}{y-1} e^{-yA(t)} (1 - e^{-A(t)})^{x-y}, \quad x \in S,$$

where

$$A(t) = \int_0^t \lambda(1 - \rho(s)) ds = -q \log \left( \frac{\eta + k^t}{\eta + 1} \right) - \int_{t^*}^{\max\{t, t^*\}} C(s) \frac{k^s \log k}{\eta + k^s} ds, \quad t \geq 0.$$

In Fig. 9 some plots of the transitions probabilities are provided for some choices of the parameters. In these cases, the probability  $P_{yx}(t)$  is decreasing with respect to  $t$  and increasing with respect to  $x$ . The conditional mean of the process is given by Eq. (19), whereas, the conditional variance is

$$Var_y(t) = y \frac{1 - \psi(t)}{\psi(t)^2}, \quad t \geq 0$$

with  $\psi(t)$  given in the first of Eqs. (16). Let us now determine some indexes of dispersion of the process which may be useful in certain applied contexts. In particular, the Fano factor is given by

$$D(t) := \frac{Var_y(t)}{E_y(t)} = \frac{1}{\psi(t)} - 1, \quad t \geq 0. \tag{20}$$

Note that  $D(t)$  is an increasing function with respect to  $t$ . From Eq. (20), it is possible to note that

- the birth process  $X(t)$  is underdispersed for  $t > \tilde{t}$  being  $\tilde{t}$  the solution of the equation  $\psi(t) = 1/2$  which has a solution when  $\tilde{\mathcal{K}}_\theta > 2y$ ;

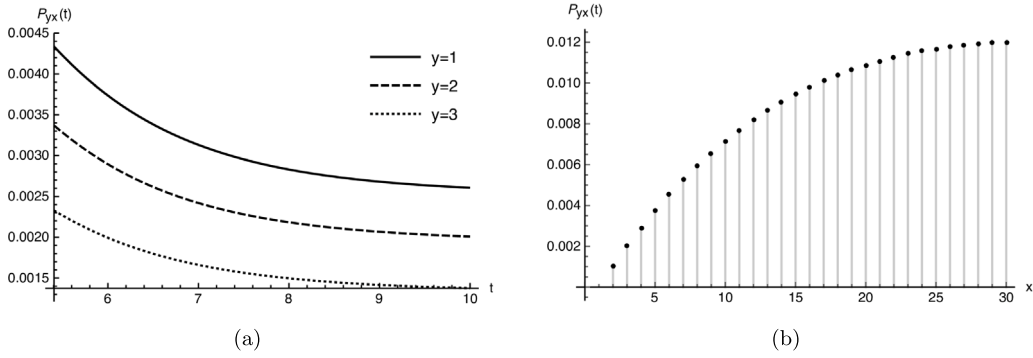


Fig. 9. The transition probabilities (a)  $P_{yx}(t)$  as a function of  $t$  for  $x = 3, 4, 5$  and (b)  $P_{yx}(t)$  as a function of  $x$  with  $t = 6$ . In both cases, we have  $C(t)$  defined in Eq. (12),  $\eta = 0.2$ ,  $m = 1$ ,  $k = 0.5$ ,  $q = 2$ ,  $p = 0.8$ ,  $y = 2$ .

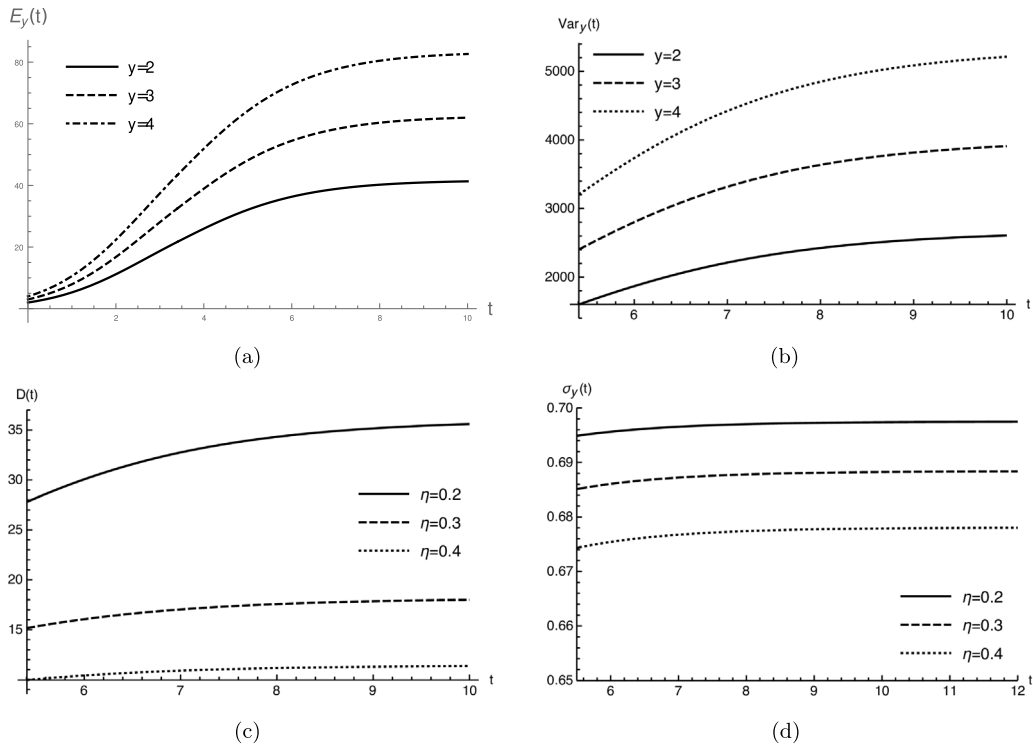


Fig. 10. (a) We consider the conditional mean  $E_y(t)$  and (b) the conditional variance  $Var_y(t)$  as a function of  $t$  with  $\eta = 0.2$ ,  $m = 1$ ,  $k = 0.5$ ,  $q = 2$ ,  $p = 0.8$ ,  $y = 2, 3, 4$ , (b) the Fano factor  $D(t)$  and (c) the coefficient of variation  $\sigma_y(t)$  as a function of  $t$  with  $m = 1$ ,  $y = 2$ ,  $k = 0.5$ ,  $q = 2$ ,  $p = 0.8$ ,  $\eta = 0.2, 0.3, 0.4$ .

- the birth process  $X(t)$  is overdispersed for  $t < \tilde{t}$ .

Similarly, one can obtain the explicit expression for the coefficient of variation  $\sigma_y(t)$  which is

$$\sigma_y(t) := \frac{\sqrt{Var_y(t)}}{E_y(t)} = \sqrt{\frac{1 - \psi(t)}{y}}, \quad t \geq 0.$$

We remark that  $\sigma_y(t)$  is increasing in  $t$  and decreasing in  $y$  and the following limits hold

$$\lim_{y \rightarrow 0^+} \sigma_y(t) = +\infty, \quad \lim_{y \rightarrow \tilde{k}_\theta} \sigma_y(t) = 0.$$

Fig. 10 provide some plots of the conditional variance  $Var_y(t)$ , of Fano factor  $D_y(t)$  and of the coefficient of variation  $\sigma_y(t)$ . All quantities represented are increasing and bounded. Note that all results presented in this section are in agreement with the birth process studied in Section 4 of Di Crescenzo and Paraggio (2019) [23] related to a logistic growth curve. The following time limits

hold

$$\begin{aligned} \lim_{t \rightarrow 0} A(t) &= 0, & \lim_{t \rightarrow +\infty} A(t) &= \log \frac{\widetilde{\mathcal{K}}_\theta}{y}, \\ \lim_{t \rightarrow 0} D(t) &= 0, & \lim_{t \rightarrow +\infty} D(t) &= \frac{\widetilde{\mathcal{K}}_\theta}{y} - 1, \\ \lim_{t \rightarrow 0} \sigma_y(t) &= 0, & \lim_{t \rightarrow +\infty} \sigma_y(t) &= \sqrt{\frac{\widetilde{\mathcal{K}}_\theta - y}{\widetilde{\mathcal{K}}_\theta y}}. \end{aligned}$$

In order to obtain a more manageable stochastic counterpart, in Section 5 we consider a particular lognormal diffusion process having the same interesting feature of the BD processes introduced so far: its mean is of type  $\widetilde{x}_\theta(t)$ .

### 5. The corresponding diffusion processes

We now consider two lognormal diffusion processes  $\{X(t); t \in I\}$  and  $\{\widetilde{X}(t); t \in I\}$ , with  $I = [t_0, +\infty)$ , having a mean which corresponds the former to the curve (1) and the latter to the curve (11). The considered non-homogeneous lognormal diffusion processes can be regarded as diffusive approximations of suitable birth–death processes having quadratic rates, as shown in Section 5.2 of Di Crescenzo et al. (2021) [24]. The stochastic differential equation (SDE) related to the classical model (1) is given by

$$dX(t) = h_\theta(t)X(t)dt + \sigma X(t)dW(t), \quad X(t_0) = X_0 \tag{21}$$

where  $W(t)$  denotes a Wiener process independent on the initial condition  $X_0$ ,  $h_\theta(t)$  is defined in Eq. (4) and  $\sigma > 0$ .

Similarly, the diffusion process  $\{\widetilde{X}(t); t \in I\}$  modeling the modified curve is the solution of the following SDE

$$d\widetilde{X}(t) = \widetilde{h}_\theta(t)\widetilde{X}(t)dt + \sigma\widetilde{X}(t)dW(t), \quad \widetilde{X}(t_0) = \widetilde{X}_0 \tag{22}$$

where  $\widetilde{h}_\theta(t)$  is defined in Eq. (10). It is worth to remark that both Eq. (21) and (22) are obtained by adding to the corresponding Malthusian equations (cf. Eq. (3)) a multiplicative noise term. The solutions of the SDEs (21) and (22) can be easily determined by means of Itô’s formula with the variable transformation  $f(\widetilde{Y}) := \log(\widetilde{Y})$ , with  $\widetilde{Y} \in \{X(t), \widetilde{X}(t)\}$ . Indeed, they are given by

$$X(t) = X_0 \exp \left( H_\xi(t_0, t) + \sigma (W(t) - W(t_0)) \right), \quad t \geq t_0, \tag{23}$$

$$\widetilde{X}(t) = \widetilde{X}_0 \exp \left( \widetilde{H}_\xi(t_0, t) + \sigma (W(t) - W(t_0)) \right), \quad t \geq t_0, \tag{24}$$

where, for  $t > s$

$$H_\xi(s, t) = q \log \frac{k^s + \eta}{k^t + \eta} - \frac{\sigma^2}{2}(t - s), \tag{25}$$

$$\widetilde{H}_\xi(s, t) = H_\xi(s, t) + \int_{\max\{s, t^*\}}^{\max\{t, t^*\}} C(u) \frac{k^u |\log k|}{\eta + k^u} du, \tag{26}$$

with  $\xi := (\theta^T, \sigma)^T = (q, k, \eta, \sigma)^T$ . The processes (23) and (24) are lognormal diffusion processes with state-space  $(0, +\infty)$  and infinitesimal moments

$$\begin{aligned} A_1(x, t) &= h_\theta(t)x, & A_2(x) &= \sigma^2 x^2 \\ \widetilde{A}_1(x, t) &= \widetilde{h}_\theta(t)x, & \widetilde{A}_2(x) &= \sigma^2 x^2, \end{aligned}$$

respectively. In Fig. 11, some simulated sample paths of the process  $\widetilde{X}(t)$  are provided by considering the function  $C(t)$  defined in Eq. (12). Clearly, the sample paths are more variable around the sample mean when  $\sigma$  is larger.

By developing a well-known strategy (cf. Román-Román et al. (2018) [13]), it is possible to get the probability distribution of  $\widetilde{X}(t)$ . More in detail, if  $\widetilde{X}_0$  follows a lognormal distribution  $A_1(\mu_0, \sigma_0^2)$  or if  $\widetilde{X}_0$  is a degenerate random variable (i.e.  $P[\widetilde{X}_0 = x_0] = 1$ , with  $x_0 > 0$ ), then the finite-dimensional distributions of the process are lognormal. Indeed, fixing  $n$  time instants  $t_1 < \dots < t_n$ , the vector  $(\widetilde{X}(t_1), \dots, \widetilde{X}(t_n))^T$  is distributed according to a  $n$ -dimensional lognormal distribution  $A_n(\epsilon, \Sigma)$ , where  $\epsilon = (\epsilon_1, \dots, \epsilon_n)^T$  with

$$\epsilon_i = \mu_0 + \widetilde{H}_\xi(t_0, t_i) = \mu_0 + q \log \frac{k^{t_0} + \eta}{k^{t_i} + \eta} + \int_{t_0}^{\max\{t_i, t_0^*\}} C(u) \frac{k^u |\log k|}{\eta + k^u} du - \frac{\sigma^2}{2}(t_i - t_0), \quad i = 1, \dots, n$$

and  $\Sigma = (\sigma_{ij})$  with

$$\sigma_{ij} = \sigma_0^2 + \sigma^2 (\min(t_i, t_j) - t_0), \quad i, j = 1, \dots, n.$$

From the case  $n = 2$ , it is possible to obtain the conditional probability distribution of the process  $\widetilde{X}(t)$ , i.e.

$$\begin{aligned} & \left[ \widetilde{X}(t) \mid \widetilde{X}(s) = x \right] \\ & \sim A_1 \left( \log x + q \log \frac{k^s + \eta}{k^t + \eta} + \int_{\max\{s, t^*\}}^{\max\{t, t^*\}} C(u) \frac{k^u |\log k|}{\eta + k^u} du - \frac{\sigma^2}{2}(t - s), \sigma^2(t - s) \right), \end{aligned} \tag{27}$$

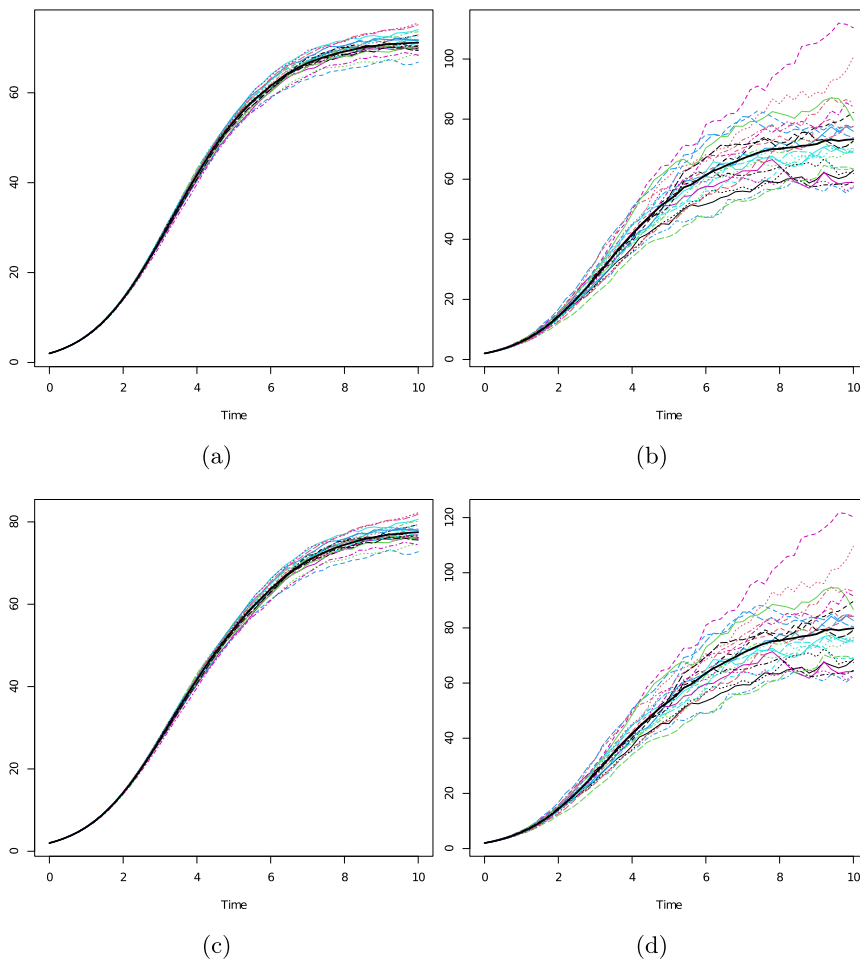


Fig. 11. 25 simulated sample paths of  $X(t)$  with (a)  $\sigma = 0.01$  and (b)  $\sigma = 0.05$  and of  $\tilde{X}(t)$  with  $C(t)$  defined in Eq. (12),  $p = 0.5$ ,  $m = 1$ , (c)  $\sigma = 0.01$  and (d)  $\sigma = 0.05$ . In all cases  $t_0 = 0$ ,  $x_0 = 2$ ,  $\eta = 0.2$ ,  $k = 0.5$ ,  $q = 2$ . The black line is the sample mean.

Table 2

The conditional and unconditional mean, mode and  $\alpha$ -percentile of  $\tilde{X}(t)$  where  $\tilde{G}^\lambda$  is defined in Eq. (28) and  $z_\alpha$  is the  $\alpha$ -percentile of the standard normal random variable.

Characteristic	Expression	$\lambda$
$E[\tilde{X}(t)^n   \tilde{X}(s) = y]$	$\tilde{G}^\lambda(t   \log y, s)$	$(n, n^2/2, 0, 1)^T$
$\text{Mode}[\tilde{X}(t)   \tilde{X}(s) = y]$	$\tilde{G}^\lambda(t   \log y, s)$	$(1, -1, 0, 1)^T$
$C_\alpha[\tilde{X}(t)^n   \tilde{X}(s) = y]$	$\tilde{G}^\lambda(t   \log y, s)$	$(1, z_\alpha, 0, 1/2)^T$
$E[\tilde{X}(t)^n]$	$\tilde{G}^\lambda(t   \mu_0, t_0)$	$(n, n^2/2, 1, 1)^T$
$\text{Mode}[\tilde{X}(t)]$	$\tilde{G}^\lambda(t   \mu_0, t_0)$	$(1, -1, 1, 1)^T$
$C_\alpha[\tilde{X}(t)^n]$	$\tilde{G}^\lambda(t   \mu_0, t_0)$	$(1, z_\alpha, 1, 1/2)^T$

for  $t > s \geq t_0$ . By employing Eq. (27), in Table 2 we provide some of the most relevant characteristics of the process making use of the following auxiliary function

$$\tilde{G}^\lambda(t | y, \tau) := \exp\left((y + \tilde{H}_\xi(\tau, t))\lambda_1 + \lambda_2(\lambda_3\sigma_0^2 + \sigma^2(t - \tau))^{\lambda_4}\right), \tag{28}$$

with  $\lambda := (\lambda_1, \lambda_2, \lambda_3, \lambda_4)^T$  and  $\tilde{H}_\xi(t)$  defined in Eq. (26).

Taking into account the expression of the quantities given in Table 2, we now get some relations between the diffusion processes  $\tilde{X}(t)$  and  $X(t)$ . Let

$$G^\lambda(t | y, \tau) := \exp\left((y + H_\xi(\tau, t))\lambda_1 + \lambda_2(\lambda_3\sigma_0^2 + \sigma^2(t - \tau))^{\lambda_4}\right),$$

with  $H_\xi(t)$  defined in Eq. (25), be the corresponding auxiliary function for the process  $X(t)$ . After some algebra, we have that

$$\frac{E[\tilde{X}(t)]}{E[X(t)]} = \exp\left(\int_{t^*}^{\max\{t,t^*\}} C(s) \frac{k^s |\log k|}{\eta + k^s} ds\right), \quad t \geq t_0, \tag{29}$$

and

$$\frac{\text{Var}[\tilde{X}(t)]}{\text{Var}[X(t)]} = \exp\left(2 \int_{t^*}^{\max\{t,t^*\}} C(s) \frac{k^s |\log k|}{\eta + k^s} ds\right), \quad t \geq t_0.$$

The above mentioned relations are useful also for estimation purposes. Indeed, in Section 6 we employ Eq. (29) for estimating the unknown function  $C(t)$ .

### 6. Parameters estimation

The model proposed in Section 5 is useful in real applications, in particular to model a Bertalanffy–Richards type growth with external modifications. To this aim, an estimation of the unknown parameters of the model is necessary. Since the distribution of  $\tilde{X}(t)$  is available in explicit form, we propose to obtain the maximum likelihood estimates (MLEs) of the parameters, following the same strategy of Di Crescenzo et al. (2022) [15]. In the following reasoning, the time instant  $t^*$  is supposed to be known, otherwise  $t^*$  needs to be estimated following the strategies described in Section 8.2. Let us consider a discrete sampling of the diffusion process  $\tilde{X}(t)$  consisting of  $d$  independent sample paths, with  $n_i$  observations for the  $i$ th sample path. Hence, the observation times are denoted by  $t_{ij}$ , for  $i = 1, \dots, d$  and  $j = 1, \dots, n_i$ . We also assume, for simplicity, that the first observation time is the same for any trajectory, i.e.  $t_{i1} = t_0$ ,  $i = 1, \dots, d$ . Moreover, let  $\tilde{\mathbf{X}} = (\tilde{\mathbf{X}}_1^T | \dots | \tilde{\mathbf{X}}_d^T)^T$  be the vector which contains all the observed states, with  $\tilde{\mathbf{X}}_i = (\tilde{X}_{i1}, \dots, \tilde{X}_{in_i})^T = (\tilde{X}(t_{i1}), \dots, \tilde{X}(t_{in_i}))^T$ . In agreement with the assumptions about  $\tilde{X}_0$  given in Section 5, we suppose that  $\tilde{X}(t_0)$  follows a lognormal distribution  $\Lambda_1(\mu_1, \sigma_1^2)$  with  $\mu_1 \in \mathbb{R}$  and  $\sigma_1^2 \in \mathbb{R}_+$ , so that the density of  $\tilde{\mathbf{X}}$  is given by

$$f_{\tilde{\mathbf{X}}}(x) = \prod_{i=1}^d \frac{\exp\left(-\frac{(\log x_{i1} - \mu_1)^2}{2\sigma_1^2}\right)}{x_{i1}\sigma_1\sqrt{2\pi}} \prod_{j=1}^{n_i-1} \frac{\exp\left(-\frac{(\log(x_{i,j+1}/x_{ij}) - \tilde{m}_\xi^{i,j+1,j})^2}{2\sigma^2 \Delta_i^{j+1,j}}\right)}{x_{ij}\sigma\sqrt{2\pi\Delta_i^{j+1,j}}}, \tag{30}$$

where  $x = (x_{1,1}, \dots, x_{1,n_1} | \dots | x_{d,1}, \dots, x_{d,n_d})^T \in \mathbb{R}_+^{n+d}$ , with  $n = \sum_{i=1}^d (n_i - 1)$ , for (cf. (26))

$$\tilde{m}_\xi^{i,j+1,j} := \tilde{H}_\xi(t_{ij}, t_{i,j+1}) = q \log \frac{k^{t_{ij}} + \eta}{k^{t_{i,j+1}} + \eta} + \int_{\max\{t_{ij}, t^*\}}^{\max\{t_{i,j+1}, t^*\}} C(u) \frac{k^u |\log k|}{\eta + k^u} du - \frac{\sigma^2}{2} (t_{i,j+1} - t_{ij}),$$

and  $\Delta_i^{j+1,j} := t_{i,j+1} - t_{ij}$  for  $i = 1, \dots, d$  and  $j = 1, \dots, n_i$ . In order to simplify the cumbersome expression of the density given in Eq. (30), we perform the following change of variables:

$$\begin{aligned} V_{0i} &:= \tilde{X}_{i1}, & i = 1, \dots, d \\ V_{ij} &:= \left(\Delta_i^{j+1,j}\right)^{-1/2} \log \frac{\tilde{X}_{i,j+1}}{\tilde{X}_{ij}}, & j = 1, \dots, n_i - 1, \quad i = 1, \dots, d. \end{aligned}$$

Therefore, by setting  $\mathbb{V} = (V_0^T | V_1^T | \dots | V_d^T)^T$  with  $V_i^T = (V_{i1}, \dots, V_{in_i})$ , the corresponding density is

$$f_{\mathbb{V}}(v) = \frac{\exp\left(-\frac{1}{2\sigma_1^2} (lv_0 - \mu_1 \mathbb{I}_d)^T (lv_0 - \mu_1 \mathbb{I}_d)\right)}{\prod_{i=1}^d v_{0i} (2\pi\sigma_1^2)^{d/2}} \cdot \frac{\exp\left(-\frac{1}{2\sigma^2} (v_{(1)} - \gamma^\xi)^T (v_{(1)} - \gamma^\xi)\right)}{(2\pi\sigma^2)^{n/2}},$$

where

$$\begin{aligned} v &= (v_0^T | v_{(1)}^T) \in \mathbb{R}^{n+d}, \quad v_0 = (v_{01}, \dots, v_{0d})^T \in \mathbb{R}^d, \quad lv_0 = (\log v_{01}, \dots, \log v_{0d})^T, \\ v_{(1)} &= (v_{11}, \dots, v_{1,n_1-1} | \dots | v_{d1}, \dots, v_{d,n_d-1})^T \in \mathbb{R}^n, \quad \mathbb{I}_d = (1, \dots, 1)^T \in \mathbb{R}^d, \end{aligned}$$

with  $\gamma^\xi = (\gamma_{11}^\xi, \dots, \gamma_{1,n_1-1}^\xi, \dots, \gamma_{d1}^\xi, \dots, \gamma_{d,n_d-1}^\xi)^T \in \mathbb{R}^n$  and  $\gamma_{ij}^\xi = \left(\Delta_i^{j+1,j}\right)^{-1/2} \tilde{m}_\xi^{i,j+1,j}$ , for  $j = 1, \dots, n_i - 1$  and  $i = 1, \dots, d$ .

By supposing that the parameters of the process,  $\xi$ , and those of the initial distribution,  $(\mu_1, \sigma_1^2)$ , are functionally independent, the log-likelihood function can be expressed as follows

$$L_{\mathbb{V}}(\xi, \mu_1, \sigma_1^2) = \tilde{L}_{\mathbb{V}}(\xi) - \frac{n+d}{2} \log 2\pi - \frac{d}{2} \log \sigma_1^2 - \sum_{i=1}^d \log v_{0i} - \frac{\sum_{i=1}^d (\log v_{0i} - \mu_1)^2}{2\sigma_1^2},$$

where

$$\tilde{L}_{\mathbb{V}}(\xi) := -\frac{n}{2} \log \sigma^2 - \frac{Z_1 + \Phi_\xi - 2\Gamma_\xi}{2\sigma^2} \tag{31}$$

and

$$Z_1 := \sum_{i=1}^d \sum_{j=1}^{n_i-1} v_{ij}^2, \quad \Phi_\xi := \sum_{i=1}^d \sum_{j=1}^{n_i-1} \frac{(\tilde{m}_\xi^{i,j+1,j})^2}{\Delta_i^{j+1,j}}, \quad \Gamma_\xi := \sum_{i=1}^d \sum_{j=1}^{n_i-1} \frac{v_{ij} \tilde{m}_\xi^{i,j+1,j}}{(\Delta_i^{j+1,j})^{1/2}}.$$

By performing the partial derivatives of the log-likelihood  $L_V$  with respect to  $\mu_1$  and  $\sigma_1^2$ , we can easily get the following MLEs:

$$\hat{\mu}_1 = \frac{1}{d} \sum_{i=1}^d \log v_{0i}, \quad \hat{\sigma}_1^2 = \frac{1}{d} \sum_{i=1}^d (\log v_{0i} - \hat{\mu}_1)^2. \tag{32}$$

In order to obtain the MLEs of  $\xi$ , we decide to adopt suitable metaheuristic optimization methods to avoid numerical problems in the resolution of the system of maximum likelihood. In addition, we need to estimate also the unknown function  $C(t)$  occurring in the definition of the modified model  $\tilde{X}(t)$ . To this aim, we assume to dispose of a data set concerning the observations of a modified Bertalanffy-Richards model  $\tilde{X}(t)$  in the time interval  $[t_0, T]$ . Consider first Eq. (29), which allows us to implement the following procedure.

**Procedure 1 - Estimation of the parameters**

**Step 1** Compute the MLEs  $\hat{\xi} = (\hat{q}, \hat{k}, \hat{\eta}, \hat{\sigma})^T$ .

**Step 2** Determine an estimation of  $t^*$ .

**Step 3** Obtain an estimation of the function  $C(t)$ .

A description of the steps of Procedure 1 is provided in the hereafter.

**Step 1** In order to determine the MLEs  $\hat{\xi}$ , we use the data over an interval  $I_t = [t_0, \bar{t}] \supset [t_0, t_I]$ , being  $\bar{t}$  a time instant quite close to  $t^*$ . For example, we can take  $\bar{t}$  as the time instant in which the spline  $S(t)$  interpolating the mean of the paths intercepts the threshold  $S$ , defined in Eq. (7).

**Step 2** To determine an estimation of  $t^*$  two different strategies are available: (i) we can use Eq. (8) and consider  $t^*$  as a parametric function of the MLEs determined at Step 1 or (ii) we can consider the mean of the first-passage-time of the estimated process (i.e. the process given in Eq. (23) obtained by considering the MLEs of the parameters) through the fixed boundary  $S$ .

**Step 3** Considering the sample mean  $E[\tilde{X}(t)]$  of the modified process (24) and the estimated mean  $\hat{E}[X(t)]$  of the classical process over the full time interval  $[t_0, T]$ , we then obtain the estimation of the function  $C(t)$  from Eq. (29) as follows

$$\hat{C}(t) = \frac{\eta + k^t}{k^t |\log k|} \frac{d}{dt} m(t), \quad t > t^*, \tag{33}$$

with  $m(t) := \log \left( \frac{E[\tilde{X}(t)]}{\hat{E}[X(t)]} \right)$ , for  $t > t^*$ . Note that since the mean of the process  $X(t)$  (cf. Eq. (23)) corresponds to the classical deterministic curve  $x_\theta(t)$  (cf. Eq. (1)), in Eq. (33) we consider

$$\hat{E}[X(t)] = E[X_0] \left( \frac{\hat{\eta} + \hat{k}^{t_0}}{\hat{\eta} + \hat{k}^t} \right)^{\hat{q}}.$$

**7. Determination of MLEs through heuristic optimization methods**

To determine the MLEs mentioned in the **Step 1** of **Procedure 1**, we develop the following reasoning.

Since the numerical methods employed to solve system of maximum likelihood may fail to converge even in the case of a quite accurate initial solution, we now propose to employ two different meta-heuristic optimization methods, namely Simulated Annealing (SA) and Ant Lion Optimizer (ALO). These two methods belong to the family of gradient-free algorithms and they are suggested when the use of the derivative of the function to be maximized is intricate. The estimation of the parameters of the initial distribution can be obtained through the explicit expressions given in Eq. (32). Hence, we need to maximize Eq. (31) on the parametric space  $\Theta = \{(q, k, \eta, \sigma) : q > 0, 0 < k < 1, \eta > 0, \sigma > 0\}$ . Since this space is continuous and unbounded, a restriction of  $\Theta$  is needed. A similar problem has been considered in Section 3.1.1 of Román-Román and Torres-Ruiz (2015) [17]. Their main idea is to find, first of all, a bounded interval  $I_q := [q_1, q_2]$  for  $q$  and from that determine sequentially two bounded intervals, the former for  $k$  and the latter for  $\eta$ . Further on, as usual, we use the interval  $I_\sigma := (0, 0.1)$  for the parameter  $\sigma$  so that the paths are compatible with a Bertalanffy-Richards type growth.

**1.1** Let us start from the determination of  $I_q$ . By interpolating the mean of the sample paths with a natural cubic spline  $S(t)$ , we find the time instant  $t_I^*$  which is the “observed” inflection instant. Then, we select  $t_1$  as the first instant in which  $S(t)/\mathcal{K}^* > e^{-1}$ , where  $\mathcal{K}^*$  is an approximation of the boundary  $S = (1+p)x_i^*$  being  $x_i^*$  the value of the curve at the observed inflection time. In this way,  $\mathcal{K}^*$  may represent an approximation of the carrying capacity of the classical Bertalanffy-Richards model. Thus, we

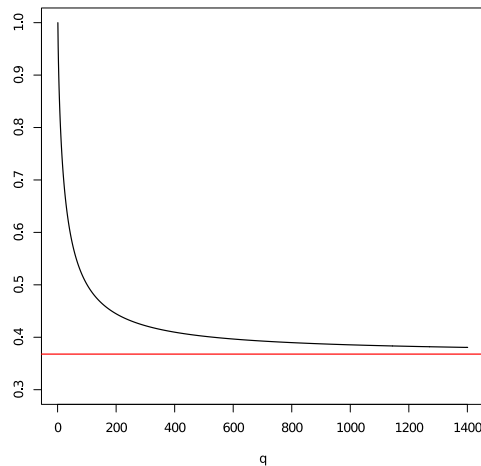


Fig. 12. The ratio  $\frac{S(t_j)}{\mathcal{K}^*}$  as a function of  $q$  (black) and the line  $y = e^{-1}$  (red).

consider the interval  $[t_1, t_2]$  where  $t_2$  is the observation instant immediately after  $t_1^*$ . Consequently, we determine the endpoints of the interval  $I_q = [q_1, q_2]$  being  $q_j$  the solutions of the following equations

$$S(t_j) = \mathcal{K}^* \left( \frac{q_j}{1 + q_j} \right)^{q_j}, \quad j = 1, 2. \tag{34}$$

1.2 We now proceed on the determination of  $I_k$  and  $I_\eta$ . From the characteristics of the classic Bertalanffy–Richards curve, we have

$$\eta = qk^{t_1}, \quad k = \left( q \left( \left( \frac{\mathcal{K}^*}{x_0} \right)^{1/q} - 1 \right) \right)^{1/(t_0 - t_1)}.$$

This allows us to consider the following functions

$$g(t, q) = \left( q \left( \left( \frac{\mathcal{K}^*}{x_0} \right)^{1/q} - 1 \right) \right)^{1/(t_0 - t)}, \quad h(q, k, t) = qk^t, \tag{35}$$

for  $q \in I_q$ ,  $t \in [t_1, t_2]$ ,  $k \in I_k \subset (0, 1)$ . From Eq. (35), it follows that the minimum value of  $g(t, q)$  is reached at  $(t_1, q_1)$  and its maximum at  $(t_2, q_2)$ . Hence, we consider for the parameter  $k$  the interval  $I_k := [k_1, k_2] = [g(t_1, q_1), g(t_2, q_2)]$ . Similarly, the function  $h(q, k, t)$  assumes its minimum value at  $(q_1, k_1, t_2)$  and its maximum at  $(q_2, k_2, t_1)$ , so that for the parameter  $\eta$  we can use the interval  $I_\eta := [\eta_1, \eta_2] = [h(q_1, k_1, t_2), h(q_2, k_2, t_1)]$ , since the function  $h(q, k, t)$  is decreasing with respect to  $t$ .

It is worth to notice that the width of the interval  $I_q$  may be too large, since small variations of the ratio  $\frac{S(t_j)}{\mathcal{K}^*}$  correspond to large variations of the parameter  $q$  (cf. Eq. (34)), as can be deduced from Fig. 12. Nevertheless, the resulting MLEs obtained via SA and ALO are quite accurate as can be noticed from the results shown in Section 8.

### 8. Simulation

In this section, we devote our analysis to a simulation study in order to validate the procedures described in Sections 6 and 7. The pattern of the simulations is based on 25 sample paths of  $\tilde{X}(t)$ , defined in Eq. (24), the time interval  $[0, 10]$  with  $q = 2$ ,  $k = 0.5$ ,  $\eta = 0.2$ ,  $\sigma \in \{0.01, 0.02\}$ . Moreover,  $C(t)$  is taken as in Eq. (12) for  $m = 1$  and where the value of  $t^*$  is obtained by setting  $p = 0.5$  in Eq. (8). The sample paths share the same length since the common observation time instants are taken as  $t_j = j \cdot 0.1$  with  $j = 0, \dots, 100$ . For the initial condition we consider a degenerate distribution centered in  $x_0 = 2$ . In the study, we suppose that the threshold  $S = (1 + p)x(t_1)$  is known, in the sense that the value of  $p$  is given. Otherwise, a set of possible values for  $p$  can be explored to select the best estimation (in terms of minimization of the absolute relative error between the sample mean and the estimated mean). Once the sample paths are simulated, we consider a sample size  $n = 51$ , being the data equally spaced in the interval under consideration. With the aim of obtaining better estimates, the steps of Procedure 1 are replicated 300 times. For any parameter, the mean of the resulting estimates is taken as the final value. As can be seen in Fig. 13, the estimates stabilize around a specific value as the number of replications increases.

For the realization of the simulation study and the application to real data, the R software has been used. Specifically, the `metaheuristicOpt` package, which implements the metaheuristic Ant Lion Optimizer algorithm, and the `GenSA` package, which contains the Simulated-Annealing algorithm. For both methods, the intervals, determined in Section 7, were given in input. Then, the initial solution of each parameter was determined by choosing a random value with a uniform distribution in any interval. The

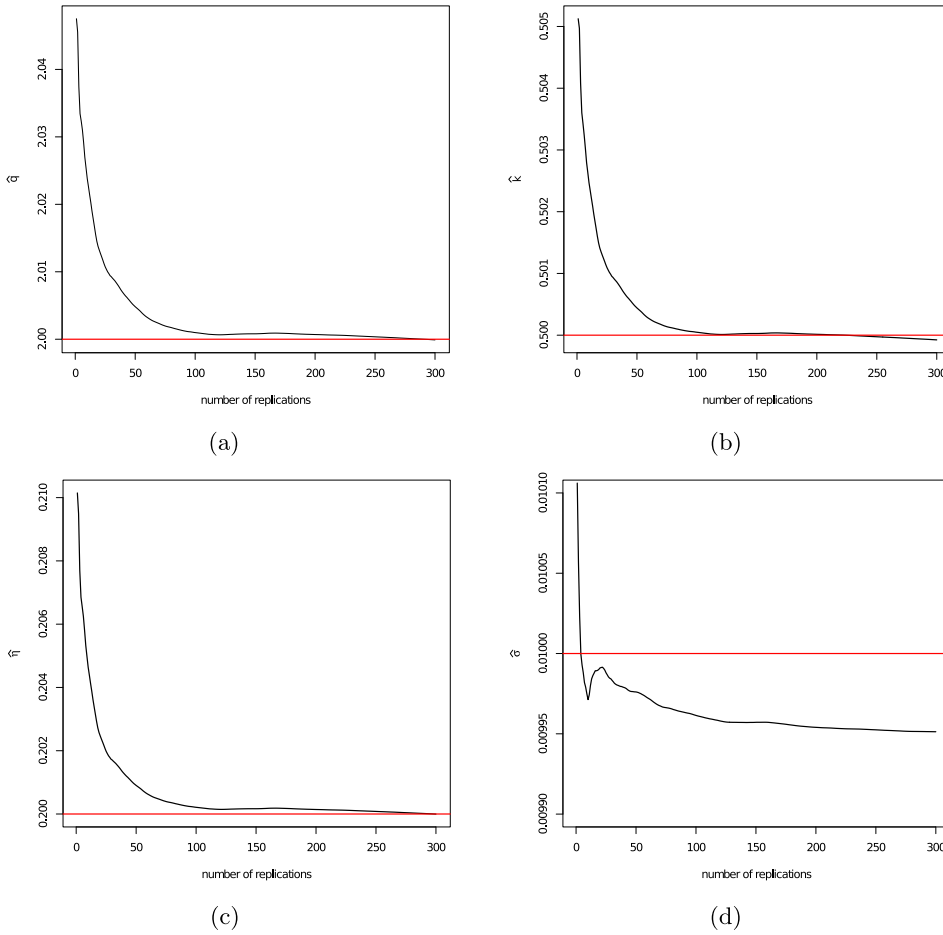


Fig. 13. Convergence of the estimates of the parameter (a)  $\hat{q}$ , (b)  $\hat{k}$ , (c)  $\hat{\eta}$ , (d)  $\hat{\sigma}$  in the case  $\sigma = 0.01$ . The red lines represent the real parameters.

Table 3

The theoretical and the observed inflection instant, and the corresponding absolute relative error (RAE).

Parameter	Theoretical inflection instant	$\sigma$	Observed inflection instant	RAE
$t_I$	3.32193	0.01	3.36223	0.01213
		0.02	3.49254	0.05136

machine used for the computations was an Apple M1, with a total of 8 cores. The time taken to obtain the results reported below with 300 replications is 1800.325 s, and with 100 replications is 582.049 s.

Let us now focus on the estimation of the parameters  $q, k, \eta, \sigma$  and of the function  $C(t)$ .

### 8.1. Step 1: Estimate of $\xi$

For any  $j = 0, \dots, 50$  we approximate the sample mean of  $\tilde{x}_i(t_j)$ ,  $i = 1, \dots, 25$ , with a natural cubic spline  $S(t)$ . Then, through its derivatives, we also determine an approximation of the observed inflection time instant. See Fig. 14 for the plot of  $\frac{d}{dt}S(t)$  and  $\frac{d^2}{dt^2}S(t)$ , and Table 3 for a comparison between the theoretical inflection point  $t_I$  and observed inflection instant.

To apply SA or ALO algorithm, we first compute the intervals  $I_\nu$  with  $\nu \in \{q, k, \eta, \sigma\}$  using the strategy described in Section 7. We remark that in this first part of the procedure the knowledge of the exact value of  $t^*$  is irrelevant since we use the data over the time interval  $[t_0, \bar{t}]$  where  $\bar{t}$  represents the time instant corresponding to the boundary  $S = (1 + p)x_j^*$ . The obtained intervals are given in Table 4. After that, we apply SA and ALO algorithms. The results, given in Table 4, show that even if the width of the intervals  $I_\nu, \nu \in \{q, k, \eta, \sigma\}$ , is large, the RAE of the resulting MLEs is small. In Table 5 we provide the MLEs obtained by considering different number of replications. We remark that the estimates are still reasonable even when the number of replications is smaller.

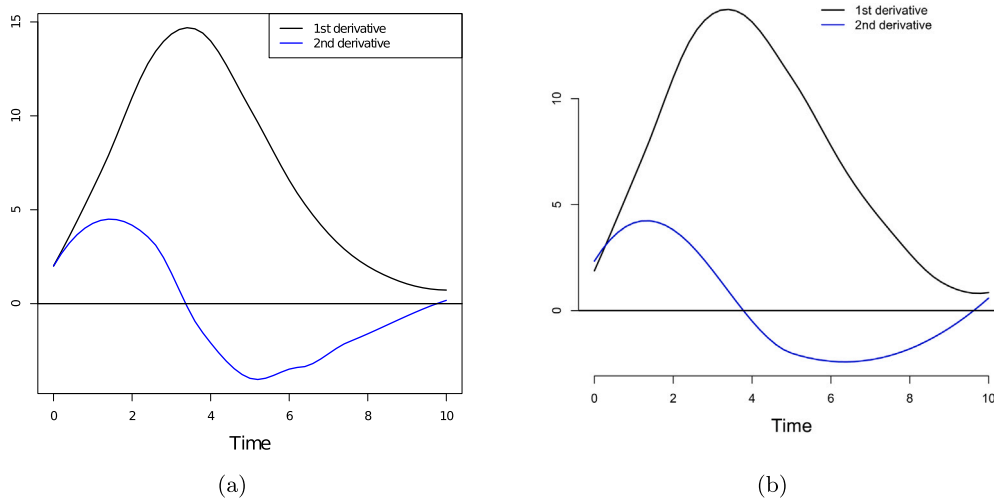


Fig. 14. The 1st and 2nd derivative of the spline  $S(t)$  for (a)  $\sigma = 0.01$  and (b)  $\sigma = 0.02$ .

Table 4

The real values, the minimum and maximum width of the bounded intervals, the MLEs (determined with SA and ALO algorithm) and the corresponding absolute relative error (RAE) of the parameters.

Parameter	Real value	min width	max width	Method	MLE	RAE
$q$	2	4.15554	5.11776	SA	1.99990	0.00005
				ALO	2.03645	0.01822
$k$	0.5	0.63553	0.67700	SA	0.49992	0.00015
				ALO	0.50340	0.00680
$\eta$	0.2	1.47345	1.97406	SA	0.19999	0.00001
				ALO	0.20703	0.03514
$\sigma$	0.01	0.1	0.1	SA	0.00995	0.00487
				ALO	0.00988	0.01200
Parameter	Real value	min width	max width	Method	MLE	RAE
$q$	2	3.78010	5.68256	SA	1.99645	0.00177
				ALO	2.08720	0.04360
$k$	0.5	0.60332	0.69750	SA	0.49942	0.00115
				ALO	0.50685	0.01370
$\eta$	0.2	1.36523	2.39929	SA	0.19941	0.00295
				ALO	0.21742	0.08710
$\sigma$	0.02	0.1	0.1	SA	0.01993	0.00337
				ALO	0.01994	0.00293

By comparing the RAE of the MLEs obtained via SA and via ALO, we note that the results obtained via SA are better than those obtained via ALO. For this reason, from now on, we adopt the MLEs obtained via SA.

8.2. Step 2: Estimate of  $t^*$

In order to compute the estimated time instant  $\hat{t}^*$ , two options are available: (i) we can use the MLEs obtained so far and compute  $\hat{t}^*$  by means of the deterministic formula given in Eq. (8), or (ii) we can compute  $\hat{t}^*$  as the mean of first-passage-time (FPT) of the estimated process (i.e. the process whose parameters are estimated by the MLEs) through the boundary  $S = (1 + p)x_i$  being  $x_i$  the observed inflection point, in agreement with Eq. (7) and  $p = 0.5$ . The results obtained by means of procedure (i) are shown in Table 6: note that the estimated time instant has an absolute relative error (RAE) equal to 1.09% for  $\sigma = 0.01$  and 1.00% for  $\sigma = 0.02$ . For the procedure (ii), as done in other similar works (cf. for instance, Di Crescenzo et al. (2022) [15]), we use the R package `fptdApprox` (see Román-Román et al. (2008) [25,26]) to approximate the FPT density of the process through the boundary  $S$ . Fig. 15 shows the approximated FPT density and the FPT location function. In Table 6 we provide the mean, the standard deviation, the mode, the 1st, the 5th and the 9th deciles of the FPT. In this case, the RAE between the estimated and the theoretical inflection time is 2.71% for  $\sigma = 0.01$  and 8.45% for  $\sigma = 0.02$ .

**Table 5**

The MLEs (determined with SA and ALO algorithm) and the corresponding absolute relative error of the parameters with different numbers of replications. The real values of  $q, k, \eta$  and  $\sigma$  are given in the first row of both the tables.

Method	No. of replications	$q = 2$	$k = 0.5$	$\eta = 0.2$	$\sigma = 0.01$
SA	30 (relative error:)	$\hat{q} = 2.00928$ (0.00464)	$\hat{k} = 0.50094$ (0.00187)	$\hat{\eta} = 0.20171$ (0.00854)	$\hat{\sigma} = 0.00998$ (0.00167)
ALO	30 (relative error:)	$\hat{q} = 2.00880$ (0.00440)	$\hat{k} = 0.50098$ (0.00195)	$\hat{\eta} = 0.20166$ (0.00831)	$\hat{\sigma} = 0.00984$ (0.01616)
SA	300 (relative error:)	$\hat{q} = 1.99990$ (0.00005)	$\hat{k} = 0.49992$ (0.00015)	$\hat{\eta} = 0.19999$ (0.00001)	$\hat{\sigma} = 0.00995$ (0.00487)
ALO	300 (relative error:)	$\hat{q} = 2.03645$ (0.00680)	$\hat{k} = 0.50340$ (0.00681)	$\hat{\eta} = 0.20703$ (0.03514)	$\hat{\sigma} = 0.00988$ (0.01200)
Method	No. of replications	$q = 2$	$k = 0.5$	$\eta = 0.2$	$\sigma = 0.02$
SA	30 (relative error:)	$\hat{q} = 2.00871$ (0.00435)	$\hat{k} = 0.50074$ (0.00148)	$\hat{\eta} = 0.20187$ (0.00934)	$\hat{\sigma} = 0.02001$ (0.00031)
ALO	30 (relative error:)	$\hat{q} = 2.02218$ (0.01109)	$\hat{k} = 0.50107$ (0.00215)	$\hat{\eta} = 0.20448$ (0.02238)	$\hat{\sigma} = 0.01999$ (0.00060)
SA	300 (relative error:)	$\hat{q} = 1.99645$ (0.00177)	$\hat{k} = 0.49942$ (0.00115)	$\hat{\eta} = 0.19941$ (0.00295)	$\hat{\sigma} = 0.01993$ (0.00337)
ALO	300 (relative error:)	$\hat{q} = 2.08720$ (0.04360)	$\hat{k} = 0.50685$ (0.01370)	$\hat{\eta} = 0.21742$ (0.08710)	$\hat{\sigma} = 0.01994$ (0.00293)

**Table 6**

The theoretical value and the estimate obtained via Procedure (i) of the time instant  $t^*$ . The mean, the mode, the 1st, the 5th and the 9th decile and the standard deviation (st. dev.) of the FPT of the approximated diffusion process through the boundary  $S = (1 + p)x_i$ , for  $p = 0.5$ . The absolute relative error of the estimates is also provided. The quantities are obtained by using SA.

Instant	th. val.	$\sigma$	Result of Proc. (i)	Mean	Mode	1st dec.	5th dec.	9th dec.	st. dev.
$t^*$	4.42611	0.01	4.47456	4.54597	4.55862	4.53713	4.43811	4.54388	0.09363
		(relative error:)	(0.01095)	(0.02708)	(0.02994)	(0.02508)	(0.00271)	(0.02661)	–
		0.05	4.47060	4.80032	4.75344	4.54871	4.78756	5.08003	0.78458
		(relative error:)	(0.01005)	(0.08455)	(0.07395)	(0.02770)	(0.08166)	(0.14774)	–

**8.3. Step 3: Estimate of  $C(t)$**

With the aim of estimating the function  $C(t)$ , we consider the mean of the stochastic process  $X(t)$  (cf. Eq. (23)) which corresponds to the classical deterministic curve  $x_\theta(t)$  (cf. Eq. (1)). The estimated function  $\hat{C}(t)$  has been obtained by means of Eq. (33), and it is plotted in Fig. 16(a)–(b). In particular, the plot shows a worsening of the estimation of  $C(t)$  for large times, as expected.

In order to have a quantitative measure of the goodness of its estimation, we have also computed the RAE between the theoretical function  $C(t)$  and the estimated function  $\hat{C}(t)$ , i.e.

$$RAE = \frac{1}{N^*} \sum_{j=1}^{N^*} \frac{|C(t_j) - \hat{C}(t_j)|}{C(t_j)},$$

where  $N^*$  denotes the number of observation times between  $\hat{t}^*$  and  $T$ . When  $\sigma = 0.01$ , we have  $RAE \simeq 0.02101$ , whereas if  $\sigma = 0.02$ , we find  $RAE \simeq 0.05775$ .

Using the estimated function  $\hat{C}(t)$ , we obtain the estimated mean  $\hat{E}[\tilde{X}(t)]$  of the modified process given in Eq. (24). Both the estimated mean and the sample mean are plotted in Fig. 16(c)–(d) and they almost coincide. Clearly, when  $t \rightarrow T$  the difference between  $C(t)$  and  $\hat{C}(t)$  is more relevant.

**9. Application to real data of oil production**

The considered model (cf. Eq. (24)) is reasonable to describe phenomena in which the growth rate may be modified starting from a specific instant by known external factors. A representative example will be considered in this section. It is concerning oil production since external causes may be effective at a certain time in order to increase the amount of extracted oil. Hence, let us consider an application of the stochastic model introduced in Section 5 to real data concerning oil production in France, taken from [27] and reported in Fig. 17(a). The amount of produced oil is measured in TWh (Terawatt per hour). We consider the time interval from 1958 (the first year in which the cumulative oil production exceeds 100 TWh) to 2016. In this case, the curve representing the yearly oil production exhibits more than one peak, as in Laherrère (2000) [28]. Our main goal is to establish that the considered model (24) is in agreement with the observed real data by following the steps of Procedure 1.

**Step 1** As illustrated in Section 8.1, we approximate the data with a natural cubic spline  $S(t)$  and we determine an approximation of the inflection time instant  $t_I$  by means of the derivatives of  $S(t)$ . The derivative of  $S(t)$  is plotted in Fig. 17(b). The approximated

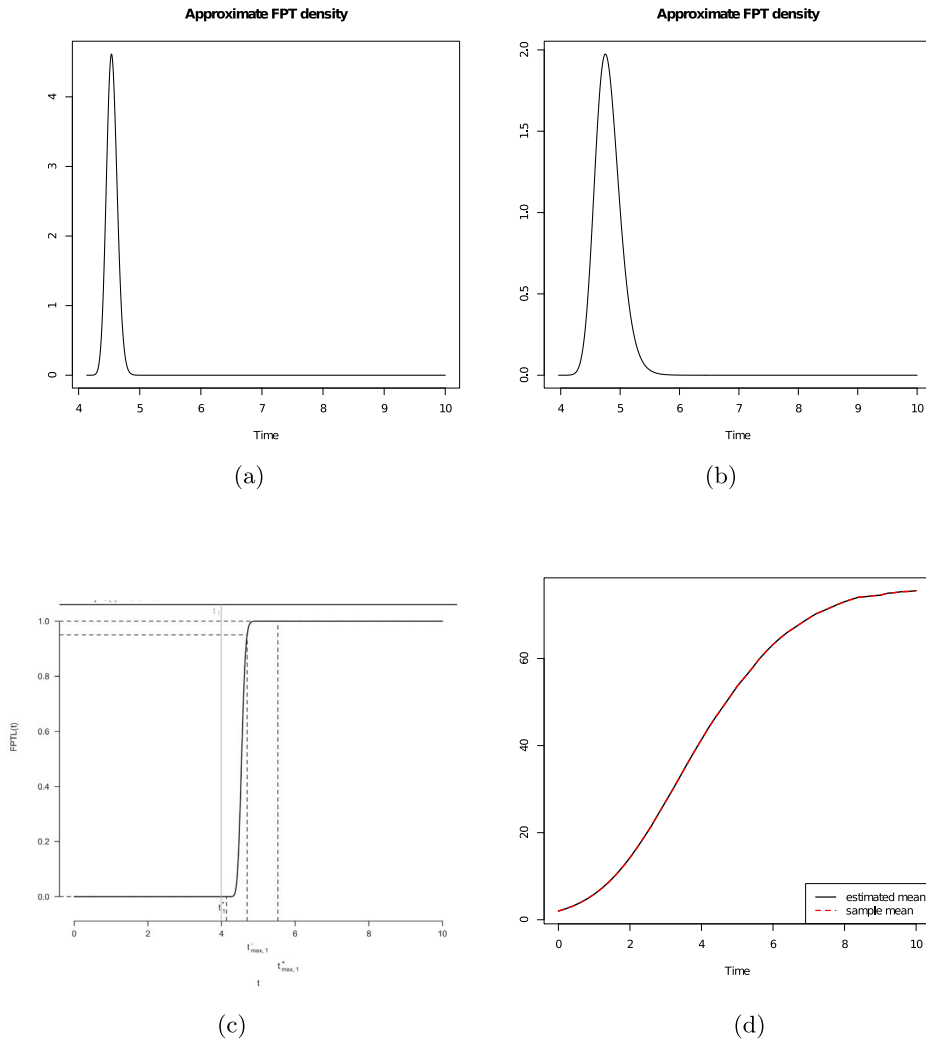


Fig. 15. The approximated FPT density function with the MLEs obtained by SA algorithm for (a)  $\sigma = 0.01$  and (c)  $\sigma = 0.02$ . The FPT location function with the MLEs obtained by SA algorithm for (b)  $\sigma = 0.01$  and (d)  $\sigma = 0.02$ .

inflection time instant is given by  $t_I \simeq 1964$ . The intervals  $I_\nu$  with  $\nu \in \{q, k, \eta, \sigma\}$  and the corresponding MLEs are given in Table 7. The MLEs have been determined by means of the data over the restricted interval  $[t_0, \bar{t}]$ , where  $\bar{t}$  is the time instant corresponding to the boundary  $S = (1 + p)x_I^*$  being  $x_I^*$  the observed inflection point and  $p > 0$ . Unlike the examples examined in the simulation study (cf. Section 8) where  $p$  was assumed to be known, we now examine the case where  $p$  is previously unknown. For estimate purposes, we consider a set of reasonable values for  $p$ . Among these, we select the value  $\hat{p}$  which finally minimizes the RAE between the estimated mean and the sample mean (see Step 3 below).

**Step 2** We compute the estimated value of  $t^*$  by means of the two available procedures: (i) using the MLEs and compute  $\hat{t}^*$  by means of the deterministic formula given in Eq. (8), or (ii) computing  $\hat{t}^*$  as the mean of the FPT of the estimated process through  $S = (1 + \hat{p})x_I^*$  (see Section 8.2 for further details). The obtained results are given in Table 8. As can be noticed, for any value of  $\hat{p}$ , the deterministic value of  $t^*$  is different whereas the mean of the FPT is almost the same. We select the deterministic FPT to estimate  $t^*$  for the results given in the simulation study (cf. Section 8). We point out that, for  $\hat{p} = 0.5$ , the specific value of the estimate  $\hat{t}^*$  is  $\hat{t}^* \simeq 1970$  (by considering the deterministic estimate of  $t^*$ ). This estimate is in agreement with new oil explorations started in 70 s as a consequence of the purpose of French government to invest in energy independence after the severe crisis emerged during those years (as reported in Lieber (1979) [29]).

**Step 3** Using the estimated function  $\hat{C}(t)$  obtained by means of Eq. (33), we compute the mean  $\hat{E}(\tilde{X}(t))$  of the modified process. The estimate  $\hat{p}$  is selected by minimizing the RAE between the estimated mean and the sample mean. As can be deduced from Table 9, in this case, we have  $\hat{p} = 0.5$  which corresponds to the boundary  $S = 1.5x_I^*$ . In Fig. 18, we show the estimated function

$$\int_{\hat{t}^*}^t \hat{C}(s) \frac{\hat{k}^s |\log \hat{k}|}{\hat{\eta} + \hat{k}^s} ds, \quad t \geq \hat{t}^* \tag{36}$$

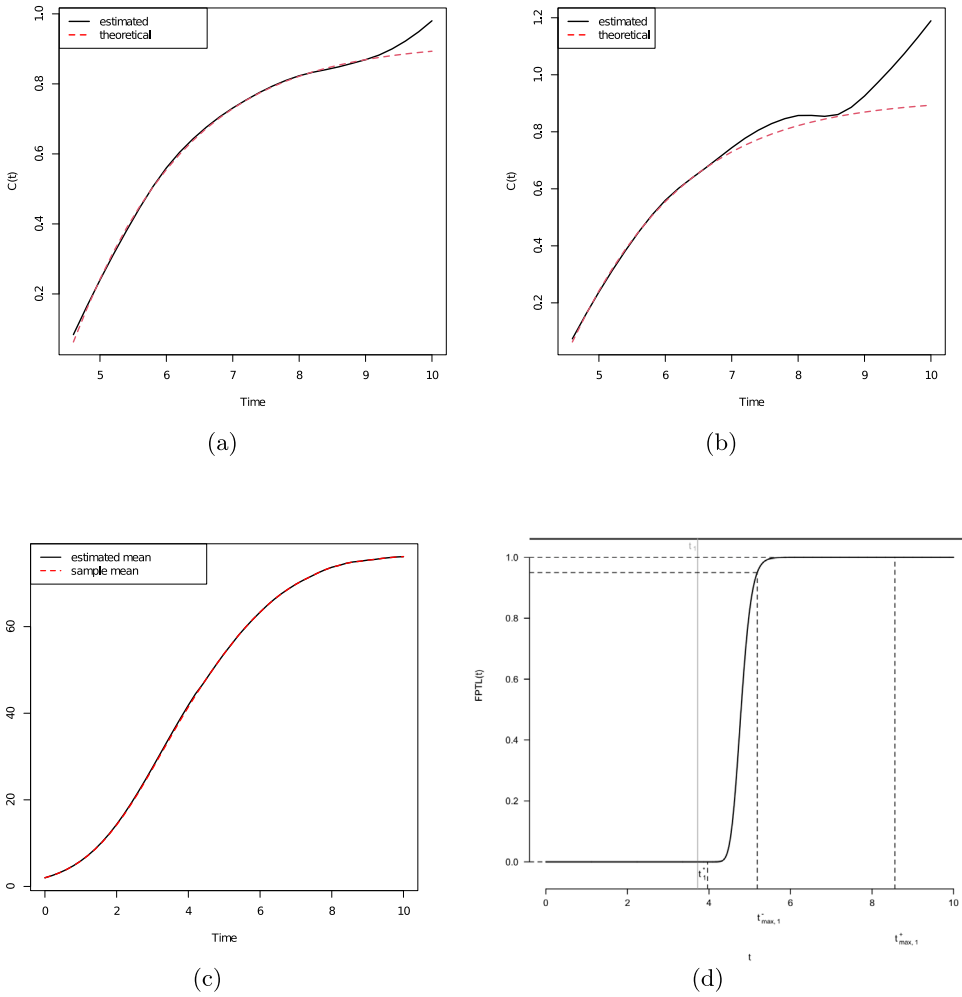


Fig. 16. The theoretical function  $C(t)$  and the estimated function  $\hat{C}(t)$  for (a)  $\sigma = 0.01$  and (c)  $\sigma = 0.02$ . The sample mean and the estimated mean for (b)  $\sigma = 0.01$  and (d)  $\sigma = 0.02$ .

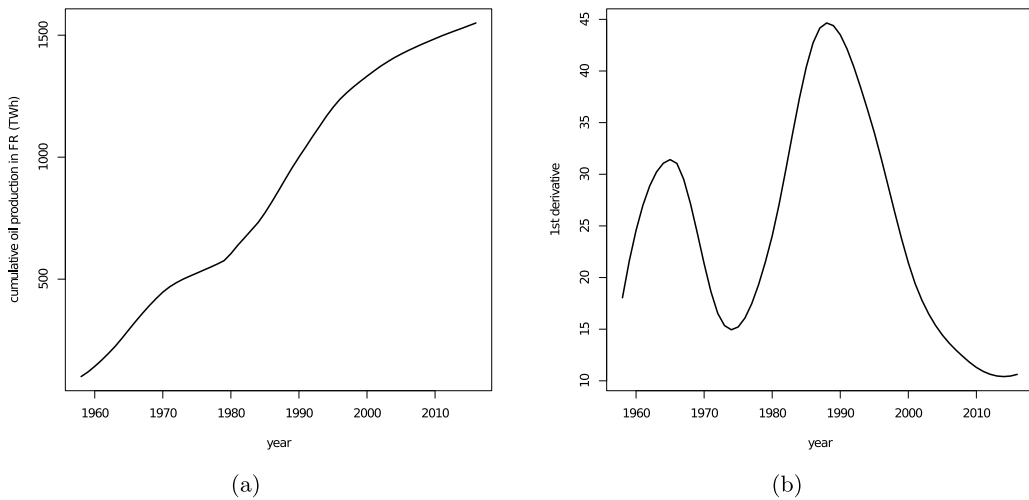


Fig. 17. (a) Cumulative oil production of France and (b) 1st derivative of the cubic spline interpolating the data between 1958 and 2016.

**Table 7**

The bounded intervals, their width and the MLEs (determined with SA) of the parameters considering different value of  $\hat{p}$ .

$\hat{p}$	Parameter	Interval	Width	MLE
0.3	$q$	$I_q = [3.16349 \cdot 10^{-2}, 2.28375]$	2.25211	0.84526
	$k$	$I_k = [4.71289 \cdot 10^{-8}, 0.94024]$	0.94024	0.78784
	$\eta$	$I_\eta = [0, 2.01897]$	2.01897	0.13325
	$\sigma$	$I_\sigma = (0, 0.1)$	0.1	0.00370
0.5	$q$	$I_q = [7.88791 \cdot 10^{-2}, 6.04903]$	6.04114	0.72390
	$k$	$I_k = [1.11653 \cdot 10^{-3}, 0.95147]$	0.95035	0.76390
	$\eta$	$I_\eta = [0, 5.47622]$	5.57622	0.10121
	$\sigma$	$I_\sigma = (0, 0.1)$	0.1	0.00359
0.7	$q$	$I_q = [2.0322 \cdot 10^{-1}, 5.43986]$	5.23664	0.71189
	$k$	$I_k = [1.63578 \cdot 10^{-1}, 0.93236]$	0.76878	0.76115
	$\eta$	$I_\eta = [6.36869 \cdot 10^{-3}, 4.40902]$	4.40265	0.09807
	$\sigma$	$I_\sigma = (0, 0.1)$	0.1	0.00325

**Table 8**

The deterministic value of the time  $t^*$ , the mean, the mode, the 1st, the 5th and the 9th decile and the standard deviation (st. dev.) of the FPT of the approximated diffusion process through the boundary  $S$  for  $t_0 = 1958$  and different values of  $\hat{p}$ .

Instant	$\hat{p}$	det. val.	Mean	Mode	1st dec.	5th dec.	9th dec.	st. dev.
$t^* - t_0$	0.3	10.59037	8.24092	8.23754	8.11223	8.24039	8.37425	0.10849
	0.5	12.29745	9.84548	9.83844	9.66999	9.84610	10.02986	0.15087
	0.7	15.68183	11.69182	11.67821	11.44741	11.68847	11.94491	0.20993

**Table 9**

The RAE between the estimated mean and the sample mean by considering different values of  $\hat{p}$ .

$\hat{p}$	0.3	0.5	0.7
RAE	0.00783%	0.00193%	0.04652%

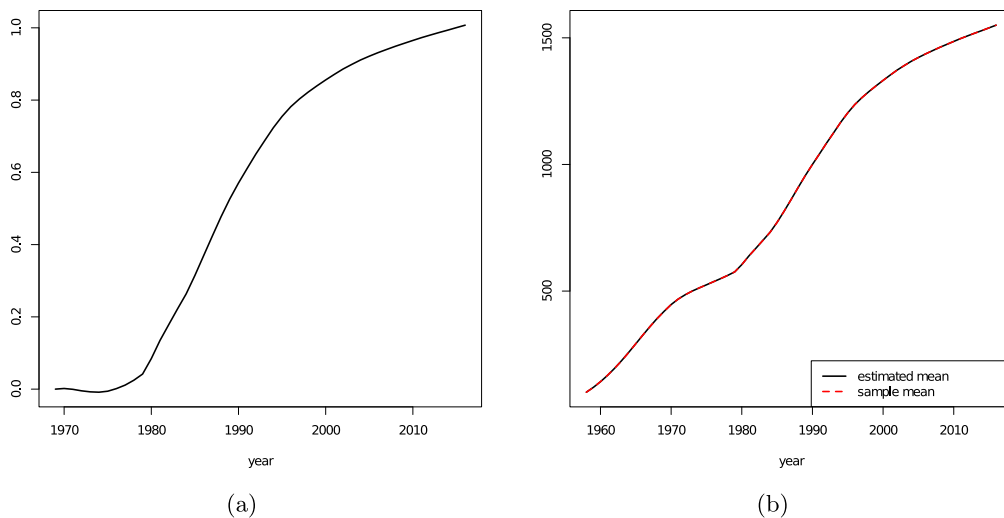


**Fig. 18.** (a) The estimated function given in Eq. (36), (b) the sample mean and the estimated mean for  $\hat{p} = 0.5$  and parameters given in Table 7.

the estimated mean and the sample mean of the data for  $\hat{p} = 0.5$ . The provided example of application confirms that the model introduced in Section 5 is appropriate for describing oil production or other phenomena with a perturbed growth rate. Moreover, as seen in this section, for particular choices of the parameters the model may describe phenomena characterized by multiple inflection points.

**10. Conclusions**

During recent years many growth models have been introduced to describe real phenomena. One of them is the Richards curve, which is a generalization of the logistic function. In detail, the main difference between the Richards model and the logistic model

is related to the ratio between the carrying capacity and the value of the curve at the inflection point. In the logistic case, this ratio is equal to  $1/2$  whereas in the Richards case it is equal to  $(1 + 1/q)^q$ . Hence, the Richards curve seems to be more reasonable to describe phenomena in which the carrying capacity is not necessarily twice the value at the inflection point. In this work, we studied a special modification of the classical Richards model. Specifically, we substitute a parameter of the classical model with a time-varying one aiming to describe situations in which the growth rate may be modified by external factors. The modification starts at a specific time instant which is identified as the first-crossing-time of the curve through a fixed boundary dependent on the value of the curve at the inflection point. The model has been described both from a deterministic and stochastic point of view. Two different kinds of stochastic processes have been introduced: birth–death processes and diffusion processes. The problems of parameters estimation and of the FPT have been also addressed. The determination of the MLEs has been conducted by means of suitable optimization methods. We considered gradient-free optimization algorithms since the expression of the derivative of the likelihood function is intricate, even if it is available in closed form. Furthermore, numerical methods have been used to determine approximations of the probability density function of the FPT of the modified process through constant boundaries.

Regarding future developments, it may be interesting to study in more detail the function  $C(t)$  and provide reasonable interpretation regarding its effects in real contexts. The model may be also enhanced to include the possibility that external factors cause a decrease of the growth rate.

### CRedit authorship contribution statement

**Antonio Di Crescenzo:** Conceptualization, Data curation, Formal analysis, Funding acquisition, Investigation, Methodology, Project administration, Resources, Software, Supervision, Validation, Visualization, Writing – original draft, Writing – review & editing. **Paola Paraggio:** Conceptualization, Data curation, Formal analysis, Funding acquisition, Investigation, Methodology, Project administration, Resources, Software, Supervision, Validation, Visualization, Writing – original draft, Writing – review & editing. **Francisco Torres-Ruiz:** Conceptualization, Data curation, Formal analysis, Funding acquisition, Investigation, Methodology, Project administration, Resources, Software, Supervision, Validation, Visualization, Writing – original draft, Writing – review & editing.

### Declaration of competing interest

The authors declare the following financial interests/personal relationships which may be considered as potential competing interests: Francisco Torres-Ruiz reports financial support was provided by Ministerio de ciencia e innovación Spain. Antonio Di Crescenzo reports financial support was provided by Government of Italy Ministry of Education University and Research. Paola Paraggio reports financial support was provided by Government of Italy Ministry of Education University and Research.

### Data availability

I have the link to data.

### Acknowledgments

A.D.C. and P.P. are members of the research group GNCS of INdAM (Istituto Nazionale di Alta Matematica). This work was supported in part by the “Ministerio de Ciencia e Innovación, Spain, under Grant PID2020-1187879GB-I00, and “María de Maeztu” Excellence Unit IMAG, reference CEX2020-001105-M, funded by MCIN/AEI/10.13039/501100011033/, and by the ‘European Union – Next Generation EU’ through MUR-PRIN 2022, project 2022XZSAFN “Anomalous Phenomena on Regular and Irregular Domains: Approximating Complexity for the Applied Sciences”, and MUR-PRIN 2022 PNRR, project P2022XSF5H “Stochastic Models in Biomathematics and Applications”.

### References

- [1] Richards FJ. A flexible growth function for empirical use. *J Exp Bot* 1959;10(2):290–301. <http://dx.doi.org/10.1093/jxb/10.2.290>.
- [2] Hiroshima T. Estimation of the gentan probability using the price of logs in private plantation forest. *J Res* 2007;12(6):417–24. <http://dx.doi.org/10.1007/s10310-007-0038-4>.
- [3] Gerhard D, Moltchanova E. A Richards growth model to predict fruit weight. *Aust N Z J Stat* 2022;64:413–21. <http://dx.doi.org/10.1111/anzs.12380>.
- [4] Matis JH, Mohammed KT, Al-Muhammed MJ. Mitigating autocorrelation in Richards growth model analysis using incremental growth data with application to turkey growth. *J Indian Soc Agric Stat* 2011;65(1):69–76.
- [5] Nahashon SN, Aggrey SE, Adefope NA, Amenyenu A, Wright D. Growth characteristics of pearl gray guinea fowl as predicted by the Richards, Gompertz, and logistic models. *Poult Sci* 2006;85(2):359–63. <http://dx.doi.org/10.1093/ps/85.2.359>.
- [6] Köhn F, Sharifi AR, Simianer H. Modeling the growth of the goettingen minipig. *J Animal Sci* 2007;85(1):84–92. <http://dx.doi.org/10.2527/jas.2006-271>.
- [7] Lv Q, Pitchford JW. Stochastic von bertalanffy models with applications to fish recruitment. *J Theoret Biol* 2007;244(4):640–55. <http://dx.doi.org/10.1016/j.jtbi.2006.09.009>.
- [8] Russo T, Baldi P, Parisi A, Magnifico G, Mariani S, Cataudella S. Lévy processes and stochastic von bertalanffy models of growth, with application to fish population analysis. *J Theoret Biol* 2009;258(4):521–9. <http://dx.doi.org/10.1016/j.jtbi.2009.01.033>.
- [9] Macêdo AMS, Brum AA, Duarte-Filho GC, Almeida FAG, Ospina R, Vasconcelos GL. A comparative analysis between a SIRD compartmental model and the Richards growth model. *Trends Comput Appl Math* 2021;22(4):545–57. <http://dx.doi.org/10.5540/tcam.2021.022.04.00545>.

- [10] Smirnova A, Pidgeon B, Chowell G, Zhao Y. The doubling time analysis for modified infectious disease Richards model with applications to COVID-19 pandemic. *Math Biosci Eng* 2022;19(3):3242–68. <http://dx.doi.org/10.3934/mbe.2022150>.
- [11] Wang XS, Wu J, Yang Y. Richards model revisited: validation by and application to infection dynamics. *J Theoret Biol* 2012;313:12–9. <http://dx.doi.org/10.1016/j.jtbi.2012.07.024>.
- [12] Asadi M, Di Crescenzo A, Sajadi FA, Spina S. A generalized Gompertz growth model with applications and related birth–death processes. *Ric Mat* <http://dx.doi.org/10.1007/s11587-020-00548-y>.
- [13] Román-Román P, Serrano-Pérez JJ, Torres-Ruiz F. Some notes about inference for the lognormal diffusion process with exogenous factors. *Mathematics* 2018;6(85). <http://dx.doi.org/10.3390/math6050085>.
- [14] Dey R, Cadigan N, Zheng N. Estimation of the von bertalanffy growth model when ages are measured with error. *J R Stat Soc Ser C Appl Stat* 2019;68(4):1131–47. <http://dx.doi.org/10.1111/rssc.12340>.
- [15] Di Crescenzo A, Paraggio P, Román-Román P, Torres-Ruiz F. Statistical analysis and first-passage-time applications of a lognormal diffusion process with multi-sigmoidal logistic mean. In: *Stat papers*. 2022. <http://dx.doi.org/10.1007/s00362-022-01349-1>.
- [16] Hole AR, Yoo HI. The use of heuristic optimization algorithms to facilitate maximum simulated likelihood estimation of random parameter logit models. *J R Stat Soc Ser C Appl Stat* 2017;66(5):997–1013. <http://dx.doi.org/10.1111/rssc.12209>.
- [17] Román-Román P, Torres-Ruiz F. A stochastic model related to the Richards-type growth curve. Estimation by means of simulated annealing and variable neighborhood search. *Appl Math Comput* 2015;266:579–98. <http://dx.doi.org/10.1016/j.amc.2015.05.096>.
- [18] Vera JF, Díaz-García JA. A global simulated annealing heuristic for the three-parameter lognormal maximum likelihood estimation. *Comput Statist Data Anal* 2008;52(12):5055–65. <http://dx.doi.org/10.1016/j.csda.2008.04.033>.
- [19] Albano G, Giorno V, Román-Román P, Román-Román S, Torres-Ruiz F. Estimating and determining the effect of a therapy on tumor dynamics by means of a modified Gompertz diffusion process. *J Theoret Biol* 2015;364:206–19. <http://dx.doi.org/10.1016/j.jtbi.2014.09.014>.
- [20] Majee S, Jana S, Khatua A, Kar TK. Growth of single species population: a novel approach. In: Banerjee S, Saha A, editors. *Nonlinear dynamics and applications*. Springer proceedings in complexity. Cham: Springer; 2022. <http://dx.doi.org/10.1007/978-3-030-99792-276>.
- [21] Albano G, Giorno V, Román-Román P, Torres-Ruiz F. Study of a general growth model. *Commun Nonlinear Sci Numer Simul* 2022;107:106110. <http://dx.doi.org/10.1016/j.cnsns.2021.106100>.
- [22] Tan WY. A stochastic Gompertz birth–death process. *Statist Probab Lett* 1986;4(1):25–8. [http://dx.doi.org/10.1016/0167-7152\(86\)90034-9](http://dx.doi.org/10.1016/0167-7152(86)90034-9).
- [23] Di Crescenzo A, Paraggio P. Logistic growth described by birth–death and diffusion processes. *Mathematics* 2019;7(6):489. <http://dx.doi.org/10.3390/math7060489>.
- [24] Di Crescenzo A, Paraggio P, Román-Román P, Torres-Ruiz F. Applications of the multi-sigmoidal deterministic and stochastic logistic models for plant dynamics. *Appl Math Model* 2021;92:884–904. <http://dx.doi.org/10.1016/j.apm.2020.11.046>.
- [25] Román-Román P, Serrano-Pérez JJ, Torres-Ruiz F. First-passage-time location function: application to determine first-passage-time densities in diffusion processes. *Comput Statist Data Anal* 2008;52:4132–46. <http://dx.doi.org/10.1016/j.csda.2008.01.017>.
- [26] Román-Román P, Serrano-Pérez JJ, Torres-Ruiz F. *Fptdapprox*: Approximation of first-passage-time densities for diffusion processes, version 2.4. 2022. <https://cran.r-project.org/web/packages/fptdApprox/>.
- [27] <https://ourworldindata.org/grapher/oil-production-by-country?country=FRA> (Accessed 16 2023).
- [28] Laherrère JH. Learn strengths, weaknesses to understand Hubbert curve. *Oil Gas J* 2000;98(16):63–76.
- [29] Lieber RJ. Europe and america in the world energy crisis. *Intern Aff* 1979;55(4):531–45. <http://dx.doi.org/10.2307/2617063>.